Epstein-Barr Virus Induced Cytidine Metabolism Roles in Transformed B-cell Growth and Survival

Jin-Hua Liang[1-4], Chong Wang[1], Stephanie Pei Tung Yiu[1-3,5], Bo Zhao[1], Rui Guo[1-3] and Benjamin E. Gewurz[1-3,5*]

[1] Division of Infectious Disease, Department of Medicine, Brigham and Women's Hospital, Harvard Medical School, Boston, MA 02115, USA

[2] Department of Microbiology, Harvard Medical School, Boston, MA 02115

[3] Broad Institute of Harvard and MIT, Cambridge, MA 02142, USA

[4] Department of Hematology, the First Affiliated Hospital of Nanjing Medical University, Jiangsu Province Hospital

[5] Graduate Program in Virology, Division of Medical Sciences, Harvard Medical School, Boston, MA 02115

*Correspondence: bgewurz@bwh.harvard.edu

Abstract:

Epstein-Barr virus (EBV) is associated with 200,000 cancers annually, including B-cell lymphomas in immunosuppressed hosts. Hypomorphic mutations of the *de novo* pyrimidine synthesis pathway enzyme cytidine 5' triphosphate synthase 1 (CTPS1) suppress cell mediated immunity, resulting in fulminant EBV infection and EBV+ central nervous system (CNS) lymphomas. Since CTP is a critical precursor for DNA, RNA and phospholipid synthesis, this observation raises the question of whether the isozyme CTPS2 or cytidine salvage pathways help meet CTP demand in EBV-infected B-cells. Here, we found that EBV upregulated CTPS1 and CTPS2 with distinct kinetics in newly infected B-cells. While CRISPR CTPS1 knockout caused DNA damage and proliferation defects in lymphoblastoid cell lines (LCL), which express the EBV latency III program observed in CNS lymphomas, double CTPS1/2 knockout caused stronger phenotypes. EBNA2, MYC and non-canonical NF-□B positively regulated CTPS1 expression. CTPS1 depletion impaired EBV lytic DNA synthesis, suggesting that latent

EBV may drive pathogenesis with CTPS1 deficiency. Cytidine rescued CTPS1/2 deficiency phenotypes in EBV-transformed LCL and Burkitt B-cells, highlighting CTPS1/2 as a potential therapeutic target for EBV-driven lymphoproliferative disorders. Collectively, our results suggest that CTPS1 and CTPS2 have partially redundant roles in EBV-transformed B-cells and provide insights into EBV pathogenesis with CTPS1 deficiency.

Key words: tumor virus, mononucleosis, chronic active EBV, gamma-herpesvirus, nucleotide metabolism, pyrimidine metabolism, gamma-herpesvirus, primary immunodeficiency, B-cell deficiency, lymphoproliferative disease

Introduction

Epstein-Barr virus (EBV) causes infectious mononucleosis and persistently infects 95% of adults worldwide. For most individuals, lifelong EBV colonization of the memory B-cell compartment is asymptomatic. Nonetheless, EBV is associated with 200,000 human cancers per year, including Burkitt lymphoma, post-transplant lymphoproliferative diseases, Hodgkin lymphoma, gastric and nasopharyngeal carcinoma (1, 2). Endemic Burkitt lymphoma caused by EBV remains the most common childhood cancer in sub-Saharan Africa (3-5).

EBV is also associated with a growing number of rare congenital immunodeficiency syndromes, in which impairment of cell mediated immune responses disrupts the host/virus balance (6, 7). Inborn errors of immunity associated with severe EBV disease include *SH2D1A* and *XIAP* mutations, which cause the X-linked lymphoproliferative diseases 1 and 2 syndromes, respectively (8). Severe EBV infection is also associated with deficiency of the MAGT1 transporter, GATA2, the IL-2-inducible T-cell kinase, the RAS guanyl-releasing protein 1 RASGRP1, CD27, CD70 and 4-1BB (6, 7, 9-13). Chronic active EBV and EBV+ lymphomas occur with gain-of-function PI3 kinase catalytic subunit mutations that cause T-cell senescence (14).

Autosomal recessive mutations of the cytidine 5' triphosphate synthetase 1 *CTPS1* gene cause a primary immunodeficiency syndrome characterized by impaired T-cell proliferation, low numbers of invariant and mucosal-associated T-cells and NK cells, and susceptibility to encapsulated bacterial and chronic viral infections, particularly by EBV and the related varicella zoster virus (15, 16). Most CTPS1 deficient patients experienced EBV disease, including severe infectious mononucleosis, chronic EBV viremia and EBV-associated primary CNS lymphomas (16). Extra-hematopoietic manifestations of CTPS1 deficiency have not been reported, and hematopoietic stem cell transplantation is curative (17).

The nucleotide cytidine is a key precursor for DNA, RNA and phospholipid biosynthesis as well as protein sialyation. Cytidine triphosphate (CTP) is maintained at the lowest concentration of cellular nucleotide pools and its synthesis is tightly regulated (18, 19). CTP is produced through *de novo* or salvage pathways. The isozymes CTPS1 and CTPS2 catalyze the ATP-dependent transfer of nitrogen form glutamine to uridine triphosphate (UTP), thereby

producing CTP and glutamate. CTPS1 and 2 share 74% amino acid sequence identity (20, 21). CTP can also be synthesized by salvage pathways, where uridine or cytidine are imported and phosphorylated by the enzymes uridine-cytidine kinase 1 or 2 (UCK1 or UCK2). Cytidine monophosphate is subsequently converted to CTP by the kinases CMPK and NDPK (**Figure 1a**). CTP synthases are the rate-limiting enzymes in *de novo* CTP synthesis (22), and CTPS1 is rapidly and highly upregulated in primary human T-cells upon T-cell receptor stimulation (23).

All patients described thus far with CTPS1 deficiency harbor a homozygous missense G-> C mutation at base 1692 of the *CTPS1* gene (rs145092287) that alters an intronic splice acceptor site. While the mutation does not alter CTPS1 catalytic activity, it causes 80-90% loss of CTPS1 protein abundance (16). The high prevalence of B-cell driven EBV-associated diseases in people with CTPS1 deficiency raises the question of how EBV-driven lymphomas arise at high frequency, despite pronounced defects in lymphocyte metabolism. Patients with CTPS1 deficiency have normal total T and B-cell numbers, though reduced frequency of memory B-cells, the site of long-term EBV persistence (16). Whether CTPS2 may have more important roles in EBV-infected B-cells than in T and NK cells, and how CTPS1 deficiency alters the latent versus lytic stages of the EBV lifecycle remain unknown.

B-cells from individuals with CTPS1 deficiency exhibit defects in proliferation (16, 23). Furthermore, the *de novo* pyrimidine synthesis enzyme DHODH inhibitor leflunomide impairs growth of EBV-driven lymphomas in murine models (24). Nonetheless, continuously growing EBV-transformed lymphoblastoid cell lines (LCLs) can be established from B-cells of patients with CTPS1 deficiency (16, 23). LCLs express the EBV latency III program also observed in primary CNS lymphomas, comprised by six Epstein-Barr nuclear antigens (EBNA) and two latent membrane proteins (LMP) that mimic signaling by the B-cell receptor and CD40 (25, 26).

To gain insights into EBV pathogenesis in the setting of CTPS1 deficiency, we characterized roles of CTPS1, CTPS2 and cytidine salvage pathways in support of EBV-transformed B-cell growth and lytic replication.

Results

EBV upregulates CTPS1 in newly infected B cells

To gain insights into EBV effects on CTPS1 and CTPS2 expression, we profiled primary human B-cells at rest and at five timepoints post infection. Whereas low levels of CTPS1 or CTPS2 were detected in resting peripheral blood CD19+ B-cells, EBV markedly upregulated both CTPS1 and CTPS2 mRNAs. CTPS1 mRNA reached maximum levels between days 4-7, the period where transforming cells undergo Burkitt-like hyper-proliferation (27, 28). By contrast, CTPS2 was progressively upregulated as newly infected cells converted to lymphoblastoid physiology between days 7-14 post-infection (**Figure 1b**). Similar effects were evident on the protein level (**Figure 1c**), where CTPS1 exhibited comparable expression patterns to Epstein-Barr nuclear antigen 2 (EBNA2) and MYC, each of which are important metabolism regulators. Using our recently published RNAseq and proteomic maps of EBV-driven B-cell growth transformation (28, 29), EBV was also found to upregulate nearly all components of the pyrimidine *de novo* and salvage pathways at similar timepoints (**Figure S1**).

CTPS1 and 2 are upregulated in primary B cells activated by combinatorial mitogenic stimuli, including by CD40-ligand (CD40L) plus interleukin-4 (IL-4), but responses to individual stimuli have not been studied (23). To cross-compare immune receptor and EBV effects on CTPS1 and CTPS2 expression, CD19+ primary B-cells were stimulated for 24 hours with CD40L, the Toll-like receptor 9 agonist CpG, □IgM, the cytokine IL-4, or combinations thereof (**Figure 1d-e**). Interestingly, CD40L or CpG alone were sufficient to upregulate CTPS1 mRNA and protein to near maximal levels, whereas CTPS2 was significantly induced on the mRNA but not protein level in response to most B-cell agonists (**Figure 1d-e**). These results highlight dynamic CTPS1 and CTPS2 regulation that varies over phases of EBV-mediated B-cell transformation and in response to particular receptor agonists.

CTPS1 is important for EBV-infected B-cell outgrowth

Since LCLs from CTPS1 deficient patients retain 10-15% CTPS1 expression, this residual CTPS1 activity may be necessary for EBV-transformed B-cell growth or survival. Alternatively, CTPS2 redundancy may support these functions. To investigate these

possibilities, we first re-analyzed data from our recent human genome-wide CRISPR/Cas9 growth and survival screen (30). Strong selection against all four single guide RNAs (sgRNAs) targeting the *CTPS1* gene was evident at screen day 21 of the LCL GM12878 and the EBV+ Burkitt cell line P3HR-1. By contrast, sgRNAs against *CTPS2* or the genes encoding pyrimidine salvage pathway enzymes UCK1 or UCK2 were not strongly selected against, suggesting that functional knockout of their targets were tolerated by these EBV-transformed B-cell lines (**Figure 2a**). Next, CRISPR mutagenesis was performed with *CTPS1* targeting sgRNAs to characterize acute CTPS1 loss-of-function effects on Burkitt and LCL proliferation (**Figure 2b**). Live cell numbers were measured at five timepoints following expression of control versus independent *CTPS1* targeting sgRNAs and puromycin selection. CTPS1 depletion significantly impaired growth of the EBV+ Burkitt cell line Daudi, which has latency I expression, and of the LCL GM12878 (**Figure 2b**). CTPS1 editing also diminished proliferation of GM11830 LCLs and Mutu I Burkitt cells (**Figure S2a-b**). A low level of proliferation was nonetheless observed in CTPS1 depleted cells, suggesting alternative routes of CTP synthesis.

To examine effects of CTPS1 depletion on B-cell survival, 7-AAD vital dye exclusion assays were performed on LCLs and Burkitt cells 5 days post sgRNA expression and puromycin selection, the timepoint at which growth curves of control and CTPS1 depleted cells diverged. Loss of CTPS1 significantly increased 7-AAD uptake in GM12878 and Daudi cells (**Figure 2c-d**) and in a second LCL and Burkitt pair (**Figure S2c-d**), indicating induction of cell death. Cell cycle analysis demonstrated that CTPS1 editing also impaired cell growth, with arrest most pronounced at the G1/S stage (**Figure 2e and Figure S2e-f**). Depletion of CTPS1 induced phosphorylation of H2AX at Ser 139 (□-H2AX), indicative of DNA damage, perhaps results from imbalance in CTP nucleotide pools. PARP cleavage was also evident, indicating apoptosis induction (**Figure 2g, Figure S2g**).

Compensatory CTPS2 role in EBV-transformed B-cell outgrowth

EBV+ CNS lymphomas are often observed in patients with CTPS1 deficiency, which are estimated to have 10-20% residual CTPS1 activity (16). Yet, the CRISPR Cancer Dependency Map (DepMap) (31) found that targeting of CTPS2 only mildly affects

proliferation of a broad range of cancer cells, including B-cell lymphomas (**Figure S3a**). These observations raise the question of the extent to which CTPS2 can be recruited to support *de novo* salvage CTP synthesis in EBV-transformed B-cells in the context of hypomorphic CTPS1 activity.

To address this question, we next tested the effects of CTPS2 editing in LCLs and Burkitt cells, alone or in the context of CTPS1 depletion. In contrast to CTPS1 depletion, CTPS2 targeting did not significantly impair LCL or Burkitt B-cell growth or survival (**Figure 3a-d, Figure S3b-d**). However, concurrent CTPS1/2 targeting nearly completely abrogated LCL outgrowth, to a greater extent than depletion of CTPS1 alone (**Figure 3a-d, Figure S3e-f**). Cytidine supplementation rescued outgrowth of CTPS1 or CTPS1/2 doubly deficient GM12878 LCLs or Daudi Burkitt cells (**Figure 3e-h**), suggesting that CRISPR effects were on target and demonstrating that the cytidine salvage pathway was capable of restoring sufficient CTP pools. Interestingly, withdrawal of exogenous cytidine at Day 7 of the proliferation assay rapidly blocked outgrowth of CTPS1 deficient and CTPS1/2 doubly-deficient GM12878 and Daudi cells (**Figure 3i-l**), further underscoring their acquired dependence on salvage CTP metabolism. CTPS1/2 depletion caused DNA damage, apoptosis induction and cell death in GM12878 and Daudi, as judged by immunoblot for cleaved-PARP, phospho □H2AX signal (**Figure 3m**). 7-AAD uptake was higher following dual CTSP1/2 targeting (**Figure 3n**).

CTPS1 Transcription upregulation in EBV-transformed B-cells

The T-cell receptor and ERK pathways are important for rapid CTPS1 expression in activated T-cells. As pathways that control B-cell CTPS1 induction remain uncharacterized, we next investigated factors important for *CTPS1* expression in EBV-transformed B-cells. First, we used our and ENCODE published LCL ChIP-seq datasets to characterize occupancy of EBV nuclear antigens and EBV LMP1-activated NF-□B transcription factors (32-34). This highlighted *CTPS1* promoter region occupancy by EBV transcription factor EBNA-LP, by multiple NF-□B transcription factor subunits, by c-MYC and MAX (**Figure 4a**). Interestingly, EBNAs 2, LP, 3A, 3C and NF-□B subunits RelB and p52 co-occupied an intergenic region ~12 kilobases downstream from the *CTPS1* promoter. RNA pol II GM12878

Chromatin Interaction Analysis by Paired-End Tag Sequencing (ChIA-PET) analysis identifies a putative long-range interaction between Pol II bound to this *CTPS1* intragenic region and the *CTPS1* promoter (35).

To study the functional significance of the EBNA and NF-□B-bound *CTPS1* intragenic region in *CTPS1* transcription regulation, we used CRISPR-interference (CRISPR-i) (36). GM12878 LCLs with endonuclease dead Cas9 fused to a KRAB transcription repressor domain were transduced with lentiviruses that express control sgRNA versus one of the twelve sgRNAs indicated in **Figure 4a**. Following puromycin selection, CRISPR-i effects on steady state *CTPS1* mRNA abundance were quantified by real time PCR. Four of the six sgRNAs targeting the putative enhancer significantly reduced CTPS1 mRNA levels. By contrast, none of the six sgRNAs targeting upstream or downstream control regions diminished CTPS1 mRNA (**Figure 4a-b**). These results suggest that the EBV latency III growth program induces *CTPS1* induction through effects at the *CTPS1* promoter and at a downstream interacting region.

EBNA2 and EBNA-LP are the first EBV proteins expressed in newly infected cells. To gain insights into potential EBNA2 roles in EBV-driven *CTPS1* induction, we infected human peripheral blood CD19+ B-cells, isolated by negative selection, with transforming B95.8 EBV, with ultraviolet (UV) inactivated B95.8, or with non-transforming P3HR-1 EBV that lacks EBNA2 and part of the EBNA-LP open reading frames. Only infection by B95.8 induced MYC, a well characterized regulator of metabolism, as well as CTPS1 by 48 hours of infection (**Figure 4c**). These data suggest that EBNA2 and/or EBNA-LP, rather than an innate immune response to the incoming viral particle, are required for CTPS1 induction in newly infected B-cells. We next used 2-2-3 LCLs with conditional EBNA2 expression, in which EBNA2 is fused to the ligand binding domain of a modified estrogen receptor that binds to 4-hydroxy-tamoxifen (4HT), to study EBNA2 roles in LCL CTPS1 expression. When grown in non-permissive conditions in the absence of 4HT for 48 hours, CTPS1 expression was rapidly lost, as was expression of EBNA2 target gene MYC (**Figure 4d**). Thus, EBNA2, perhaps together with its host target genes, are important for EBV-driven CTPS1 induction.

To characterize putative CTPS1 induction roles of the key host EBNA2 target MYC, we used p493-6 LCLs, which carry conditional 4HT-controlled EBNA2 and tetracycline-repressed

MYC alleles (37). EBNA2 inactivation by 4HT withdrawal again caused loss of CTPS1 and MYC expression in cells cultured with doxycycline to suppress exogenous *MYC* (**Figure 4e**). Interestingly, induction of exogenous MYC expression by doxycycline withdrawal restored CTPS1 expression in the absence of EBNA2 activity (**Figure 4e**). Similarly, MYC knockout in GM12878 blocked CTPS1 expression at a timepoint prior to induction of cell death (**Figure 4f**), further supporting a key role for MYC in CTPS1 regulation and providing a potential route for CTPS1 induction in Burkitt cells.

The EBV-encoded CD40 mimic LMP1 activates the NF-□B canonical and non-canonical pathways to trigger nuclear translocation of the five NF-□B transcription factor subunits. Since GM12878 ChIP-seq identified *CTPS1* locus occupancy by all NF-□B subunits, we used CRISPR to individually test their roles in LCL CTPS1 expression (**Figure 4g**). Depletion of RelB, p50 and p52 each significantly reduced CTPS1 steady-state mRNA levels (**Figure 4h**), implicating the non-canonical NF-□B pathway. In support, a □B kinase (IKK)-□-selective antagonist did not visibly reduce CTPS1 protein levels at a dose where the canonical pathway is selectively blocked, but impaired CTPS1 expression at a higher dose that also blocks the kinase IKK□, which controls the non-canonical pathway (**Figure 4i**). By contrast, ERK inhibition by an antagonist that blunts T-cell CTPS1 expression (23) failed to reduce CTPS1 expression, in spite of LMP1's ability to activate ERK (**Figure 4j**). Thus, distinct mechanisms that control CTPS1 expression in EBV+ B-cells versus T-cells.

EBV+ B-cells use *de novo* and salvage UTP metabolism

Uracil monophosphate (UMP), a key precursor in *de novo* CTP synthesis, can be synthesized from L-glutamine and L-aspartate by the sequential enzymatic activities of CAD, DHODH and UMPS. UMP can also be produced by UCK1 or UCK2 phosphorylation of imported uridine (**Figure 1a**). Interestingly, UCK was originally identified as a B-cell factor that associates with EBNA3A, suggesting possible roles in EBV-driven B-cell proliferation (38). To gain insights into potential DHODH versus UCK1/2 roles in newly infected primary B-cells, immunoblot analysis was performed on extracts from cells prior to and at five timepoints post-EBV infection. UCK2 was robustly induced by day 4, whereas DHODH expression was suppressed by day 10, despite each being induced on the mRNA level (**Figure 5a, Figure**

S4a-b). By comparison, UCK1, 2 and DHODH mRNAs were upregulated by multiple primary B-cell stimuli, while again UCK2 but not DHODH was upregulated on the protein level (**Figure 5b, Figure S4c).**

DHODH inhibition prevents EBV lymphomas in a humanized mouse model (24). We next used CRISPR to test the effects of DHODH depletion in LCLs or Burkitt cells. In media containing undialyzed fetal bovine serum (FBS), which contains uridine (**Figure 1a**), independent DHODH sgRNAs impaired proliferation of both LCLs and of Mutu I, but not Daudi Burkitt cells (**Figure 5c-f**). To more closely examine the ability of EBV-transformed B-cells to use uridine as a substrate for *de novo* CTP synthesis, control and DHODH edited LCL and BL were grown with dialyzed FBS lacking uridine. In this context, DHODH depletion more strongly inhibited proliferation, which was rescued by uridine add-back (**Figure 5g-j, Figure S5a-d).** Thus, LCLs can use amino acid *de novo* or uridine salvage for CTP synthesis (**Figure 1a**).

We next used CRISPR to test the effects of UCK1 and/or UCK2 depletion on EBV-transformed B-cell proliferation. Successful CRISPR editing of UCK2 was confirmed by immunoblot, whereas UCK1 editing was confirmed by T7 E1 assay, as we were unable to find a suitable immunoblot antibody. Unexpectedly, depletion of UCK1, UCK2 or UCK1/2 did not significantly impair GM12878 LCL or Burkitt cell proliferation (**Figure 5k-l**, **Figure S5e**). These results suggest that LCLs and Burkitt cells can synthesize sufficient CTP *de novo* when sufficient glutamine and aspartate are available, but that they are nonetheless able to switch to uridine salvage when necessary.

CTPS1 roles in EBV lytic DNA replication

Knowledge remains incomplete of how EBV remodels CTP synthesis pathways in support of the B-cell lytic cycle, where the viral immediate early transcription factors BZLF1 and BRLF1 induce early genes responsible for viral DNA replication and subsequently expression of viral late genes. Lytic replication results in synthesis of hundreds to thousands of EBV ~170 kilobase genomes by the viral DNA polymerase (39). To test *de novo* cytidine roles in EBV lytic replication, control or *CTPS1* targeting sgRNAs were expressed in EBV+ Akata Burkitt cells, a model for EBV lytic replication. Following CRISPR editing, lytic

283 replication was induced by B-cell receptor cross-linking for 24 hours. Interestingly, while
284 CTPS1 depletion did not appreciably affect expression of the immediate early gene BZLF1 or
285 early gene BMRF1, production of lytic EBV genomes was significantly impaired by
286 independent CTPS1 sgRNAs (**Figure 6a**). Lytic EBV genome replication was rescued by
287 cytidine add-back, suggesting that either the *de novo* or salvage CTP pathways can support
288 the viral lytic cycle (**Figure 6b**). Similar results were obtained in P3HR-1 Burkitt cells, in which
289 lytic replication was induced by a conditional *BZLF1* allele together with sodium butyrate
290 (**Figure 6c-d**).
291
292 **Discussion**
293 The ability of B and T lymphocytes to rapidly switch from a quiescent state into rapidly
294 growing blasts upon antigen receptor and co-receptor stimulation underlies adaptive
295 immunity. CTPS1 is highly induced by T-cell stimulation through the ERK pathway and is
296 necessary for rapid T-cell proliferation and the control of acute EBV infection (23). Yet, with
297 hypomorphic CTPS1 activity, patients often exhibit severe infectious mononucleosis, chronic
298 active EBV and EBV+ CNS B-cell lymphomas. Since EBV relies on host metabolism
299 pathways to convert newly infected cells into hyperproliferating blasts and to support lytic
300 replication, these clinical observations raise the question of how individuals with CTPS1
301 deficiency exhibit elevated EBV viral loads and frequent B-cell lymphomas, despite
302 hypoactivity of a key CTP generation enzyme, yet high CTP demands of B-cell growth (16,
303 23). Further adding to this question, classic studies indicate that CTP synthase activity is
304 frequently upregulated in cancer (40).
305 We therefore tested the effects of CTPS1, CTPS2 and CTP salvage pathways to
306 support EBV-infected B-cell growth, survival and EBV lytic replication. EBV-mediated B-cell
307 growth transformation proceeds through a genetically encoded process that proceeds
308 through Burkitt-like hyperproliferation and lymphoblastoid phases, whose physiology
309 resembles the Burkitt and LCL cell lines used in this study (28, 40). LCLs are an established
310 tissue culture model for immunoblastic lymphomas of immunosuppressed hosts. The results
311 presented here suggest that while CTPS1 activity is important for EBV-transformed B-cell
312 proliferation, cells can also utilize CTPS2 activity and cytidine salvage metabolism to support

CTP synthesis for DNA, RNA phosphatidylcholine and phosphatidylserine needs. While knowledge of cytidine concentrations in tonsil and lymphoid tissues remains limited, robust deoxycytidine kinase activity is evident in human tonsil tissue (41).

We speculate that in patients with CTPS1 deficiency, CTPS2 compensation is insufficient for cell-mediated control of EBV infection, but is nonetheless able to support EBV+ B-cell growth, together with hypomorphic CTPS1. Given our findings that CTPS2 supports proliferation of EBV-transformed CTPS1 deficient B-cells, we speculate that CTPS2 plays important roles in the CNS lymphomas observed clinically. Consequently, CTPS1/2 may serve as a therapeutic synthetic lethal target in this setting, for instance if cytidine replacement fails to restore anti-tumor immunity. While our quantitative proteomic analyses identified that CTPS1 is approximately four times more abundant than CTPS2 in primary human B-cells undergoing EBV-mediated growth transformation (28), EBV-infected lymphomas may compensate for CTPS1 deficiency by increasing CTPS2 levels and/or activity. It would be of interest to test this hypothesis through RNAseq and enzymatic profiling of CNS lymphoma samples.

CTPS1 and CTPS2 are each highly regulated at the post-translational level, including by assembly into filaments called cytoophidium that regulate catalytic activity (42-44). Whether cytoophidium form in EBV-infected B-cells generally or with CTPS1 deficiency is unknown. Furthermore, cryo-EM studies recently identified a novel filament-based mechanism of CTPS2 regulation that stabilizes nucleotide levels (45). Filaments containing CTPS1/2 and IMPDH, the rate limiting enzyme in *de novo* GTP synthesis have also been described (46), and may play important roles in EBV-infected B-cell metabolism.

CTP salvage pathways may also play important roles in support of pathogenic B-cell roles in CTPS1 deficient patients. Cytidine is imported into the CNS by nucleoside transporters located at the blood-brain barrier (47). That CTPS1/2 deficient LCL growth could be restored by cytidine supplementation highlights the potentially important role of the CTP salvage pathway in B-cells with the viral latency III program observed in CNS lymphoma. Interestingly, since oral intake may alter CNS pyrimidine levels (47), dietary cytidine and uridine restriction could potentially have antineoplastic effects in CTPS1 deficient patients with CNS lymphoma.

Patients with CTPS1 deficiency often have elevated EBV genome copy number, which may result from latent or lytic states with impaired T-cell surveillance (48). Viral lytic gene expression has been associated with EBV lymphomagenesis (49-51). Interestingly, the DHODH chemical inhibitor teriflunomide blocks EBV lytic gene expression and DNA replication (24). Here, we found that CTPS1 knockout instead reduces EBV lytic DNA replication, without impairing immediate early and early gene expression. Consistent with a potential role in supplying CTP for lytic genome synthesis, cytidine supplementation rescued EBV lytic DNA replication, newly identifying their ability to utilize cytidine salvage metabolism. It will be of interest to define relative CTPS1 and CTPS2 roles in epithelial cell EBV lytic replication.

CTP levels increase in EBV-transforming B-cells, though to lower magnitude than other deoxynucleotide triphosphates (52). Feedback and allosteric regulation renders CTPS1 activity sensitive to the levels of all four nucleotides (22, 53). EBNA2 and MYC are important regulators of EBV-driven one-carbon metabolism and purine nucleotide synthesis in newly infected cells (28). Thus, their roles in CTPS1 induction likely coordinates pools of all four deoxynucleotides to avoid imbalances and DNA damage. Indeed, CRISPR knockout of CTPS1 resulted in □□H2AX phosphorylation. While NF-□B is not required for initial EBV-driven B-cell growth (54), it is essential for LCL growth and survival, where we found a non-canonical NF-□B role in CTPS1 expression. Our findings also suggest that hyper-active MYC activity is also sufficient to drive CTPS1 expression and likely supports CTPS1 expression in Burkitt cells. By contrast, ERK and SRC have obligatory roles in robust CTPS1 upregulation upon T-cell activation that are critical for T-cell expansion (**Figure 7**). Notably, MYC has key roles in *de novo* pyrimidine nucleotide synthesis (55).

In summary, these studies highlight that multiple CTP synthesis pathways are operative in EBV-infected B-cells, and that each can play important roles in EBV transformed B-cell growth and lytic DNA replication. Collectively, these results highlight CTP synthesis pathways as important therapeutic targets in EBV-driven lymphoproliferative disorders.

Methods

CRISPR/Cas9 gene editing. CRISPR editing was performed as previously described (56).

Briefly, Broad Institute pXPR-011 pXPR-515 control sgRNA, Avana or Brunello library sgRNAs, as listed in **Supplementary Table 1**, were cloned into lentiGuide-Puro (Addgene Cat#52963) or pLenti SpBsmBI sgRNA Hygro (Addgene Cat# 62205). sgRNA expressing lentiviruses were produced by 293T transfection and used to transduce LCLs or Burkitt cells with stably expressed Cas9.

Growth Curve Analysis. Cells were normalized to the same starting concentration. Cell numbers were then quantified, using the Cell Titer Glo assays at the indicated times.

Recombinant EBV. EBV B95-8 virus was produced from B95-8 cells with conditional BZLF1 expression. The P3HR-1 EBV strain was produced from P3HR-1 cells with conditional BZLF1 and BRFL1 expression. UV irradiation of B95-8 virus supernatants was performed at a cumulative intensity of 3J per square centimeter on ice, to prevent heat-induced virus degradation. The quantitation of equal infection of B95-8, UV B 95-8 and P3HR1 was performed as previously described (57).

Statistical Analysis. Data are presented as means ± standard errors of the means. Data were analyzed using analysis of variance (ANOVA) with Sidak's multiple-comparison test or two-tailed paired Student's *t* test with Prism7 software. For all statistical tests, a *P* cutoff value of <0.05 was used to indicate significance.

Acknowledgements

This work was supported by NIH RO1s AI137337 and CA228700 (BEG) and a Burroughs Wellcome Career Award in Medical Sciences and CA047006 to BZ. We thank Jaap Middeldorp for generously sharing multiple anti-EBV antibodies.

Compliance with ethical standards

Conflict of interest BG receives research funding from Abbvie unrelated to this study.

Author contributions

J.L. performed the experiments. C.W, R.G., S.Y., B.Z. provided technological assistance. R.G. performed bioinformatic analysis. J.L, R.G. and B.E.G. prepared the manuscript. B.E.G supervised the study.

Disclosure of Conflicts of Interest

The authors declare no competing interests

References

1. Farrell PJ. 2019. Epstein-Barr Virus and Cancer. Annu Rev Pathol 14:29-53.
2. Pei Y, Wong JH, Robertson ES. 2020. Herpesvirus Epigenetic Reprogramming and Oncogenesis. Annu Rev Virol 7:309-331.
3. Giulino-Roth L, Goldman S. 2016. Recent molecular and therapeutic advances in B-cell non-Hodgkin lymphoma in children. Br J Haematol 173:531-44.
4. Ozuah NW, Lubega J, Allen CE, El-Mallawany NK. 2020. Five decades of low intensity and low survival: adapting intensified regimens to cure pediatric Burkitt lymphoma in Africa. Blood Adv 4:4007-4019.
5. Gopal S, Gross TG. 2018. How I treat Burkitt lymphoma in children, adolescents, and young adults in sub-Saharan Africa. Blood 132:254-263.
6. Tangye SG, Latour S. 2020. Primary immunodeficiencies reveal the molecular requirements for effective host defense against EBV infection. Blood 135:644-655.
7. Cohen JI. 2015. Primary Immunodeficiencies Associated with EBV Disease. Curr Top Microbiol Immunol 390:241-65.
8. Latour S, Winter S. 2018. Inherited Immunodeficiencies With High Predisposition to Epstein-Barr Virus-Driven Lymphoproliferative Diseases. Front Immunol 9:1103.
9. Lenardo M, Lo B, Lucas CL. 2016. Genomics of Immune Diseases and New Therapies. Annu Rev Immunol 34:121-49.
10. Latour S, Fischer A. 2019. Signaling pathways involved in the T-cell-mediated immunity against Epstein-Barr virus: Lessons from genetic diseases. Immunol Rev 291:174-189.
11. Ghosh S, Kostel Bal S, Edwards ESJ, Pillay B, Jimenez Heredia R, Erol Cipe F, Rao G, Salzer E, Zoghi S, Abolhassani H, Momen T, Gostick E, Price DA, Zhang Y, Oler AJ, Gonzaga-Jauregui C, Erman B, Metin A, Ilhan I, Haskologlu S, Islamoglu C, Baskin K, Ceylaner S, Yilmaz E, Unal E, Karakukcu M, Berghuis D, Cole T, Gupta AK, Hauck F, Kogler H, Hoepelman AIM, Baris S, Karakoc-Aydiner E, Ozen A, Kager L, Holzinger D, Paulussen M, Kruger R, Meisel R, Oommen PT, Morris E, Neven B, Worth A, van Montfrans J, Fraaij PLA, Choo S, Dogu F, Davies EG, Burns S, et al. 2020. Extended clinical and immunological phenotype and transplant outcome in CD27 and CD70 deficiency. Blood 136:2638-2655.
12. Somekh I, Thian M, Medgyesi D, Gulez N, Magg T, Gallon Duque A, Stauber T, Lev A, Genel F, Unal E, Simon AJ, Lee YN, Kalinichenko A, Dmytrus J, Kraakman MJ, Schiby G, Rohlfs M, Jacobson JM, Ozer E, Akcal O, Conca R, Patiroglu T, Karakukcu M, Ozcan A, Shahin T, Appella E, Tatematsu M, Martinez-Jaramillo C, Chinn IK, Orange JS, Trujillo-Vargas CM, Franco JL, Hauck F, Somech R, Klein C, Boztug K. 2019. CD137 deficiency causes immune dysregulation with predisposition to lymphomagenesis. Blood 134:1510-1516.
13. Platt CD, Fried AJ, Hoyos-Bachiloglu R, Usmani GN, Schmidt B, Whangbo J, Chiarle R, Chou J, Geha RS. 2017. Combined immunodeficiency with EBV positive B cell lymphoma and epidermodysplasia verruciformis due to a novel homozygous mutation in RASGRP1. Clin Immunol 183:142-144.
14. Lucas CL, Kuehn HS, Zhao F, Niemela JE, Deenick EK, Palendira U, Avery DT, Moens L, Cannons JL, Biancalana M, Stoddard J, Ouyang W, Frucht DM, Rao VK,

Atkinson TP, Agharahimi A, Hussey AA, Folio LR, Olivier KN, Fleisher TA, Pittaluga S, Holland SM, Cohen JI, Oliveira JB, Tangye SG, Schwartzberg PL, Lenardo MJ, Uzel G. 2014. Dominant-activating germline mutations in the gene encoding the PI(3)K catalytic subunit p110delta result in T cell senescence and human immunodeficiency. Nat Immunol 15:88-97.

15. Notarangelo LD. 2013. Functional T cell immunodeficiencies (with T cells present). Annu Rev Immunol 31:195-225.
16. Martin E, Minet N, Boschat AC, Sanquer S, Sobrino S, Lenoir C, de Villartay JP, Leite-de-Moraes M, Picard C, Soudais C, Bourne T, Hambleton S, Hughes SM, Wynn RF, Briggs TA, Genomics England Research C, Patel S, Lawrence MG, Fischer A, Arkwright PD, Latour S. 2020. Impaired lymphocyte function and differentiation in CTPS1-deficient patients result from a hypomorphic homozygous mutation. JCI Insight 5.
17. Nademi Z, Wynn RF, Slatter M, Hughes SM, Bonney D, Qasim W, Latour S, Truck J, Patel S, Abinun M, Flood T, Hambleton S, Cant AJ, Gennery AR, Arkwright PD. 2019. Hematopoietic stem cell transplantation for cytidine triphosphate synthase 1 (CTPS1) deficiency. Bone Marrow Transplant 54:130-133.
18. Higgins MJ, Graves PR, Graves LM. 2007. Regulation of human cytidine triphosphate synthetase 1 by glycogen synthase kinase 3. J Biol Chem 282:29493-503.
19. Traut TW. 1994. Physiological concentrations of purines and pyrimidines. Mol Cell Biochem 140:1-22.
20. Kursula P, Flodin S, Ehn M, Hammarstrom M, Schuler H, Nordlund P, Stenmark P. 2006. Structure of the synthetase domain of human CTP synthetase, a target for anticancer therapy. Acta Crystallogr Sect F Struct Biol Cryst Commun 62:613-7.
21. van Kuilenburg AB, Meinsma R, Vreken P, Waterham HR, van Gennip AH. 2000. Isoforms of human CTP synthetase. Adv Exp Med Biol 486:257-61.
22. Kassel KM, Au da R, Higgins MJ, Hines M, Graves LM. 2010. Regulation of human cytidine triphosphate synthetase 2 by phosphorylation. J Biol Chem 285:33727-36.
23. Martin E, Palmic N, Sanquer S, Lenoir C, Hauck F, Mongellaz C, Fabrega S, Nitschke P, Esposti MD, Schwartzentruber J, Taylor N, Majewski J, Jabado N, Wynn RF, Picard C, Fischer A, Arkwright PD, Latour S. 2014. CTP synthase 1 deficiency in humans reveals its central role in lymphocyte proliferation. Nature 510:288-92.
24. Bilger A, Plowshay J, Ma S, Nawandar D, Barlow EA, Romero-Masters JC, Bristol JA, Li Z, Tsai MH, Delecluse HJ, Kenney SC. 2017. Leflunomide/teriflunomide inhibit Epstein-Barr virus (EBV)- induced lymphoproliferative disease and lytic viral replication. Oncotarget 8:44266-44280.
25. Saha A, Robertson ES. 2019. Mechanisms of B-Cell Oncogenesis Induced by Epstein-Barr Virus. J Virol 93.
26. Shannon-Lowe C, Rickinson AB, Bell AI. 2017. Epstein-Barr virus-associated lymphomas. Philos Trans R Soc Lond B Biol Sci 372.
27. Nikitin PA, Yan CM, Forte E, Bocedi A, Tourigny JP, White RE, Allday MJ, Patel A, Dave SS, Kim W, Hu K, Guo J, Tainter D, Rusyn E, Luftig MA. 2010. An ATM/Chk2-mediated DNA damage-responsive signaling pathway suppresses

Epstein-Barr virus transformation of primary human B cells. Cell Host Microbe 8:510-22.

28. Wang LW, Shen H, Nobre L, Ersing I, Paulo JA, Trudeau S, Wang Z, Smith NA, Ma Y, Reinstadler B, Nomburg J, Sommermann T, Cahir-McFarland E, Gygi SP, Mootha VK, Weekes MP, Gewurz BE. 2019. Epstein-Barr-Virus-Induced One-Carbon Metabolism Drives B Cell Transformation. Cell Metab 30:539-555 e11.
29. Wang C, Li D, Zhang L, Jiang S, Liang J, Narita Y, Hou I, Zhong Q, Zheng Z, Xiao H, Gewurz BE, Teng M, Zhao B. 2019. RNA Sequencing Analyses of Gene Expression during Epstein-Barr Virus Infection of Primary B Lymphocytes. J Virol 93.
30. Ma Y, Walsh MJ, Bernhardt K, Ashbaugh CW, Trudeau SJ, Ashbaugh IY, Jiang S, Jiang C, Zhao B, Root DE, Doench JG, Gewurz BE. 2017. CRISPR/Cas9 Screens Reveal Epstein-Barr Virus-Transformed B Cell Host Dependency Factors. Cell Host Microbe 21:580-591 e7.
31. Tsherniak A, Vazquez F, Montgomery PG, Weir BA, Kryukov G, Cowley GS, Gill S, Harrington WF, Pantel S, Krill-Burger JM, Meyers RM, Ali L, Goodale A, Lee Y, Jiang G, Hsiao J, Gerath WFJ, Howell S, Merkel E, Ghandi M, Garraway LA, Root DE, Golub TR, Boehm JS, Hahn WC. 2017. Defining a Cancer Dependency Map. Cell 170:564-576 e16.
32. Zhao B, Barrera LA, Ersing I, Willox B, Schmidt SC, Greenfeld H, Zhou H, Mollo SB, Shi TT, Takasaki K, Jiang S, Cahir-McFarland E, Kellis M, Bulyk ML, Kieff E, Gewurz BE. 2014. The NF-kappaB genomic landscape in lymphoblastoid B cells. Cell Rep 8:1595-606.
33. Jiang S, Zhou H, Liang J, Gerdt C, Wang C, Ke L, Schmidt SCS, Narita Y, Ma Y, Wang S, Colson T, Gewurz B, Li G, Kieff E, Zhao B. 2017. The Epstein-Barr Virus Regulome in Lymphoblastoid Cells. Cell Host Microbe 22:561-573 e4.
34. Ernst J, Kheradpour P, Mikkelsen TS, Shoresh N, Ward LD, Epstein CB, Zhang X, Wang L, Issner R, Coyne M, Ku M, Durham T, Kellis M, Bernstein BE. 2011. Mapping and analysis of chromatin state dynamics in nine human cell types. Nature 473:43-9.
35. Tang Z, Luo OJ, Li X, Zheng M, Zhu JJ, Szalaj P, Trzaskoma P, Magalska A, Wlodarczyk J, Ruszczycki B, Michalski P, Piecuch E, Wang P, Wang D, Tian SZ, Penrad-Mobayed M, Sachs LM, Ruan X, Wei CL, Liu ET, Wilczynski GM, Plewczynski D, Li G, Ruan Y. 2015. CTCF-Mediated Human 3D Genome Architecture Reveals Chromatin Topology for Transcription. Cell 163:1611-27.
36. Wang LW, Trudeau SJ, Wang C, Gerdt C, Jiang S, Zhao B, Gewurz BE. 2018. Modulating Gene Expression in Epstein-Barr Virus (EBV)-Positive B Cell Lines with CRISPRa and CRISPRi. Curr Protoc Mol Biol 121:31 13 1-31 13 18.
37. Schuhmacher M, Kohlhuber F, Holzel M, Kaiser C, Burtscher H, Jarsch M, Bornkamm GW, Laux G, Polack A, Weidle UH, Eick D. 2001. The transcriptional program of a human B cell line in response to Myc. Nucleic Acids Res 29:397-406.
38. Kashuba E, Kashuba V, Sandalova T, Klein G, Szekely L. 2002. Epstein-Barr virus encoded nuclear protein EBNA-3 binds a novel human uridine kinase/uracil phosphoribosyltransferase. BMC Cell Biol 3:23.
39. Kenney SC, Mertz JE. 2014. Regulation of the latent-lytic switch in Epstein-Barr virus. Semin Cancer Biol 26:60-8.

40. Williams JC, Kizaki H, Weber G, Morris HP. 1978. Increased CTP synthetase activity in cancer cells. Nature 271:71-3.
41. Szyfter K, Sasvari-Szekely M, Spasokukotskaja T, Antoni F, Staub M. 1985. Pyrimidine salvage enzymes in human tonsil lymphocytes: II. Purification and properties of deoxycytidine kinase. Acta Biochim Biophys Acad Sci Hung 20:173-82.
42. Chang CC, Keppeke GD, Sung LY, Liu JL. 2018. Interfilament interaction between IMPDH and CTPS cytoophidia. FEBS J 285:3753-3768.
43. Carcamo WC, Satoh M, Kasahara H, Terada N, Hamazaki T, Chan JY, Yao B, Tamayo S, Covini G, von Muhlen CA, Chan EK. 2011. Induction of cytoplasmic rods and rings structures by inhibition of the CTP and GTP synthetic pathway in mammalian cells. PLoS One 6:e29690.
44. Lynch EM, Hicks DR, Shepherd M, Endrizzi JA, Maker A, Hansen JM, Barry RM, Gitai Z, Baldwin EP, Kollman JM. 2017. Human CTP synthase filament structure reveals the active enzyme conformation. Nat Struct Mol Biol 24:507-514.
45. Lynch EM, Kollman JM. 2020. Coupled structural transitions enable highly cooperative regulation of human CTPS2 filaments. Nat Struct Mol Biol 27:42-48.
46. Keppeke GD, Chang CC, Peng M, Chen LY, Lin WC, Pai LM, Andrade LEC, Sung LY, Liu JL. 2018. IMP/GTP balance modulates cytoophidium assembly and IMPDH activity. Cell Div 13:5.
47. Cansev M. 2006. Uridine and cytidine in the brain: their transport and utilization. Brain Res Rev 52:389-97.
48. Hislop AD, Taylor GS, Sauce D, Rickinson AB. 2007. Cellular responses to viral infection in humans: lessons from Epstein-Barr virus. Annu Rev Immunol 25:587-617.
49. Munz C. 2019. Latency and lytic replication in Epstein-Barr virus-associated oncogenesis. Nat Rev Microbiol 17:691-700.
50. Ma SD, Yu X, Mertz JE, Gumperz JE, Reinheim E, Zhou Y, Tang W, Burlingham WJ, Gulley ML, Kenney SC. 2012. An Epstein-Barr Virus (EBV) mutant with enhanced BZLF1 expression causes lymphomas with abortive lytic EBV infection in a humanized mouse model. J Virol 86:7976-87.
51. Ma SD, Hegde S, Young KH, Sullivan R, Rajesh D, Zhou Y, Jankowska-Gan E, Burlingham WJ, Sun X, Gulley ML, Tang W, Gumperz JE, Kenney SC. 2011. A new model of Epstein-Barr virus infection reveals an important role for early lytic viral protein expression in the development of lymphomas. J Virol 85:165-77.
52. Hafez AY, Messinger JE, McFadden K, Fenyofalvi G, Shepard CN, Lenzi GM, Kim B, Luftig MA. 2017. Limited nucleotide pools restrict Epstein-Barr virus-mediated B-cell immortalization. Oncogenesis 6:e349.
53. Endrizzi JA, Kim H, Anderson PM, Baldwin EP. 2005. Mechanisms of product feedback regulation and drug resistance in cytidine triphosphate synthetases from the structure of a CTP-inhibited complex. Biochemistry 44:13491-9.
54. Price AM, Tourigny JP, Forte E, Salinas RE, Dave SS, Luftig MA. 2012. Analysis of Epstein-Barr virus-regulated host gene expression changes through primary B-cell outgrowth reveals delayed kinetics of latent membrane protein 1-mediated NF-kappaB activation. J Virol 86:11096-106.

55. Huang M, Graves LM. 2003. De novo synthesis of pyrimidine nucleotides; emerging interfaces with signal transduction pathways. Cell Mol Life Sci 60:321-36.
56. Greenfeld H, Takasaki K, Walsh MJ, Ersing I, Bernhardt K, Ma Y, Fu B, Ashbaugh CW, Cabo J, Mollo SB, Zhou H, Li S, Gewurz BE. 2015. TRAF1 Coordinates Polyubiquitin Signaling to Enhance Epstein-Barr Virus LMP1-Mediated Growth and Survival Pathway Activation. PLoS Pathog 11:e1004890.
57. Wang LW, Wang Z, Ersing I, Nobre L, Guo R, Jiang S, Trudeau S, Zhao B, Weekes MP, Gewurz BE. 2019. Epstein-Barr virus subverts mevalonate and fatty acid pathways to promote infected B-cell proliferation and survival. PLoS Pathog 15:e1008030.

Figure Legends

Figure 1. Upregulation of *de novo* CTP synthesis enzymes CTPS1 and CTPS2 in primary human B-cells stimulated by EBV or B-cell agonists.

(A) Schematic diagram of *de novo* and salvage CTP synthesis pathways. The *de novo* pathway synthesizes CTP from L-glutamine and L-aspartate or uridine substrates, whereas the salvage pathway uses cytidine for CTP synthesis.

(B) Quantitative PCR (qPCR) analysis of CTPS1 and CTPS2 mRNA levels in primary human CD19+ peripheral blood B-cells infected by EBV B95.8 strain for the indicated days.

(C) Immunoblot analysis of CTPS1, CTPS2, MYC, EBNA2 and load control DDX1 levels in whole cell lysate (WCL) from primary human CD19+ peripheral blood B-cells infected by the EBV B95.8 strain for the indicated days.

(D) qPCR analysis CTPS1 and CTPS2 mRNA levels in primary human CD19+ B-cells stimulated for 24 hours by Mega-CD40 ligand (CD40L, 50ng/mL), the toll-receptor 9 agonist CpG (1μM), □IgM crosslinking (1μg/mL), interleukin 4 (IL-4, 20ng/mL) or combinations thereof, as indicated.

(**E**) Immunoblot analysis of CTPS1, CTPS2 and DDX1 abundances in WCL of primary human CD19+ B-cells stimulated for 24 hours by CD40 ligand Meda-CD40L (50ng/mL), CpG (1μM), □IgM (1μg/mL), IL- 4 (20ng/mL), or combinations thereof, as indicated.

For d and d, mean and SEM values from n=3 replicates are shown. *, $p<0.05$; **, $p<0.01$; ***, $p<0.001$; ****, $p<0.0001$; ns, non-significant using one way Anova with multiple comparisons. For c and d, representative blots from n=3 replicates are shown.

Figure 2. CTPS1 roles in EBV transformed B-cell growth and survival.

(A) Distribution of Avana human genome-wide CRISPR screen sgRNA Log2 fold-change values at Day 21 versus input in Cas9+ P3HR-1 Burkitt lymphoma (BL) left or GM12878 LCL (right). Values for CTPS1, CTPS2, UCK1 or UCK2 targeting sgRNAs (red lines) are overlaid on gray gradients depicting all Avana sgRNA library values (30). Average Day 21 vs input values from four screen biological replicates are shown.

(**B**) Immunoblot analysis (top) and growth curve analysis (bottom) of Cas9+ GM12878 LCLs or Daudi Burkitt lymphoma (BL) expressing non-targeting control (C) or independent sgRNAs against *CTPS1*. WCL were obtained at day 7 post sgRNA expression. Growth curves were begun at 96 hours post-sgRNA expression and 48 hours post-puromycin selection.

(C) Flow cytometry (FACS) analysis of vital dye 7-AAD uptake in GM12878 LCL at Day 7 post-expression of control or sgRNAs targeting *CTPS1*. Shown at right are median + SEM values from n=3 replicates.

(**D**) FACS analysis of 7-AAD uptake in Daudi BL at Day 7 post-expression of control or *CTPS1* targeting sgRNAs. Shown at right are median + SEM values from n=3 replicates.

(**E**) Propidium iodide cell cycle analysis of GM12878 LCL (left) or Daudi BL (right) expressing control or CTPS1 sgRNAs at Day 7.

(**F**) Immunoblot (top) and growth curve analysis (bottom) of GM12878 or Daudi expressing control or independent sgRNAs against CTPS2. WCL were obtained at day 5 post sgRNA expression. Growth curves were begun at 96 hours post-sgRNA expression and 48 hours post-puromycin selection.

(**G**) Immunoblot analysis of WCL from GM12878 or Daudi, 7 days post expression of control or CTPS1 sgRNAs.

For B, C, D, E and F, mean and SEM values from n=3 replicates are shown. *, $p<0.05$; **, $p<0.01$; ***, $p<0.001$; ****, $p<0.0001$; ns, non-significant using one way Anova with multiple comparisons. For B, F and G, representative blots or n=3 replicates are shown.

Figure 3. Partially redundant CTPS1/2 roles in EBV-transformed B cell growth and survival.

(A) Immunoblot of WCL from GM12878 LCL on Day 7 post expression of the indicated control, CTPS1 and/or CTPS2 sgRNAs.

(B) Growth curve analysis of GM12878 LCL with control, CTPS1 and/or CTPS2 sgRNAs, as indicated.

(C) Immunoblot of WCL from Daudi BL Day 7 post expression of the indicated control, CTPS1 and/or CTPS2 sgRNAs.

(D) Growth curve analysis of Daudi BL with control, CTPS1, and/or CTPS2 sgRNAs, as indicated.

(E-H) Growth curve analysis of GM12878 LCL (E-F) or Daudi BL (G-H) that express control, CTPS1 or CTPS1 and CTPS2 sgRNAs as indicated, with 200 □M cytidine supplementation.

(I-L) Growth curve analysis of GM12878 (I), GM11830 (J), Daudi (K) or Mutu I (L) with CTPS1 sgRNA expression, cultured in the presence of 200 □M cytidine from days 1-7 or throughout.

(M) Immunblot analysis of WCL from GM12878 (left) or Daudi (right) at Day 7 post expression of the indicated sgRNAs.

(**N**) Mean + SEM values of FACS 7-AAD values from GM12878 (left) or Daudi (right) expressing the indicated sgRNAs for 7 days from n=3 replicates.

Blots in A, C, and M are representative of n=3 replicates. Growth curves were begun at 96 hours post-sgRNA expression and 48 hours post-puromycin selection. Growth curves show mean + SEM fold change live cell numbers from n = 3 replicates. *, $p<0.05$; **, $p<0.01$; ***, $p<0.001$; ****, $p<0.0001$; ns, non-significant using one way Anova with multiple comparisons.

Figure 4. CTPS1 Transcription Regulation in EBV-infected B-cells.

(A) Chromatin immunoprecipitation (ChIP)-sequencing (ChIP-seq) tracks for the indicated transcription factors or histone 3 lysine 27 acetyl (H3K27Ac) at the LCL *CTPS1* locus. Y-axis ranges are indicated for each track. Also shown below is LCL RNA Pol II ChIA-PET signal indicating a long-range DNA interaction between the *CTPS1* promoter region and an intronic site. Schematic diagram of the *CTPS1* locus shown below, with exons indicated by rectangles. CRISPR-i sgRNA targeting sites are shown.

(B) Normalized CTPS1 mRNA levels in dCAS9-KRAB+ GM12878 expressing the indicated sgRNAs for CRISPR-i analysis for 5 days. CTPS1 mRNA level in cells with non-targeting control sgRNA was set to 1.

(C) Immunoblot of WCL from primary human B-cells that were either mock-infected or infected with equal amounts of the non-transforming P3HR-1, UV-irradiated B95-8 or B95-8 EBV strain for four days.

(D) Immunoblot analysis of samples prepared from 2-2-3 EBNA2-HT LCLs grown in the absence (EBNA2 non-permissive) or presence (EBNA2 permissive) of 4HT (1 μM) for 48 hours.

(E) Immunoblot analysis of WCL from conditional P493-6 LCLs treated with 1 ug/ml doxycycline (DOX) to suppress exogenous *MYC* allele expression and/or with 1 □M 4HT to induce EBNA2 activity for 48 hours, as indicated.

(F) Immunoblot analysis of WCL from GM12878 LCL expressing control or independent *MYC*-targeting sgRNAs for 5 days, as indicated.

(G) Immunoblot analysis of WCL from GM12878 LCL expressing the indicated sgRNA for 6 Days.

(**H**) qPCR analysis of CTPS1 and CTPS2 mRNA levels in GM12878 LCL expressing the indicated sgRNAs for 7 days. Levels in cells with sgControl were set to 1.

(**I**) Immunoblot of WCL from GM12878 or GM11830 LCLs treated with the indicated concentrations of the IKK antagonist Calbiochem VIII for 48 hours. 1 □M selectively blocks the canonical pathway IKK□ kinase.

(**J**) Immunoblot of WCL from GM12878 or GM11830 LCLs treated with the ERK inhibitor PD0325901 at the indicated concentrations for 48 hours.

Blots in C, D, E, F, G, I and J are representative of n = 3 experiments. SEM + Mean values are shown in B and H from n=3 replicates. *, $p < 0.05$; **, $p < 0.01$; ***, $p<0.001$ using one way Anova with multiple comparisons.

Figure 5. De novo pyrimidine synthesis enzyme DHODH and uridine salvage roles in EBV-transformed B-cell growth.

(A) Immunoblot analysis of UCK2, DHODH and load-control DDX1 levels in whole cell lysate

(WCL) from human CD19+ peripheral blood B-cells infected by the EBV B95.8 strain for the indicated days.

(**B**) Immunoblot analysis of UCK1, DHODH and DDX1 abundances in primary human CD19+ B-cells stimulated for 24 hours by CD40L (50ng/mL), CpG (1μM), □IgM (1μg/mL), IL-4 (20ng/mL), or combinations thereof, as indicated.

(C-F) Immunoblot analysis (top) and growth curve analysis (bottom) of GM12878 (C), GM11830 (D), Mutu I (E) and Daudi (F) expressing non-targeting control or independent sgRNAs against *DHODH* in media containing 10% undialyzed fetal bovine serum (FBS). WCL were obtained at day 7 post sgRNA expression.

(G-J) Growth curve analysis of GM12878 (G), GM11830 (H), Mutu I (I) and Daudi (J) expressing control or independent sgRNAs against DHODH. Cells were grown in media containing dialyzed FBS and supplemented with 200 □M uridine where indicated.

(K) Growth curve analysis (left) and immunoblot of WCL or T7 endonuclease I **(**T7E1) assays of CRISPR editing of the *UCK1* locus (right) from GM12878 expressing the indicated sgRNAs.

(L) Growth curve analysis (left) and immunoblot of WCL or T7E1 assays of CRISPR editing of the *UCK1* locus (right) from Daudi expressing the indicated sgRNAs.

Blots in A-F, K and L are representative of n = 3 experiments. SEM + Mean values are shown in C-L from n=3 replicates. *, $p < 0.05$; **, $p < 0.01$; ***, $p<0.001$; ns, non-significant using one way Anova with multiple comparisons.

Figure 6. Key CTPS1 role in EBV lytic DNA replication

(A) Immunoblot analysis of WCE from EBV+ Akata BL expressing the indicated sgRNAs for 96 hours and mock-induced or induced for lytic replication by □IgG (10 □g/ml) cross-linking for 24 hours. Blots for immediate early BZLF1 and early BMRF1 lytic antigens, CTPS1 and GADPH are shown. Shown below are EBV genome copy numbers determined by qPCR analysis. Values for mock-induced cells with sgControl were set to 1. Relative intracellular EBV DNA copy numbers were determined by qPCR using primers to the *BALF5* gene and were normalized for input cell number using primers to *GAPDH*.

(**B**) Immunoblots and qPCR analysis of EBV genome copy number as in panel A, from cells grown in the presence of 200 □M cytidine rescue.

(C) Immunoblot analysis of WCE from Cas9+ P3HR-1 Burkitt cells expressing a conditional 4-HT regulated BZLF1 allele and the indicated sgRNAs, mock-induced or induced for EBV lytic reactivation by addition of 400nM 4HT and 500□M sodium butyrate for 24 hours. sgRNAs were expressed for 6 days. Blots for EBV-encoded wildtype BZLF1 and BMRF1 as well as for CTPS1 and GADPH are shown. Shown below are qPCR analysis of EBV genome copy number, as in A.

(**D**) Immunoblots and qPCR analysis of EBV genome copy number as in panel C from cells grown in the presence of 200 □M cytidine rescue.

Blots in A-D are representative of n=3 replicates. Mean + SEM values from n=3 of biologically independent replicates are shown in A-D. ****, $p<0.0001$; ***$p<0.001$; NS, non-significant using one way Anova with multiple comparisons.

Figure 7. Schematic model of CTPS1 roles in T vs EBV-infected B-cells.

T-cell receptor stimulation induces CTPS1 expression, at least in part through the ERK and SRC pathways. By contrast, EBV induces CTPS1 in LCLs through EBNA2, MYC and LMP1-activated non-canonical NF-□B pathway, whereas hyper-expressed MYC has key roles in Burkitt CTPS1 induction. CTPS1 and CTPS2 activity together supply CTP pools for EBV-transformed B-cells to prevent nucleotide imbalance, DNA damage, cell cycle arrest and apoptosis. CTPS1 depletion also impairs EBV lytic DNA replication.

Supplementary Figure Legends

Figure S1. EBV-induced *de novo* pyrimidine synthesis pathway expression.

(A-F) CAD (A), DHODH (B), UMPS (C) CMPK1 and CMPK2 (D), CTPS1 and CTPS2 (E), NME1 and NME2 encoded NDPK (F) relative protein abundances (top) and mRNA abundances (bottom) over the first 28 days of peripheral blood CD19+ B-cell infection by EBV B95.8 at a multiplicity of infection of 0.1. Mean + SEM values from n=4 tandem-mass-tag-based proteomic and n=3 RNAseq replicates were used for these analyses and were obtained from recently published datasets (28, 29). *, $p<0.05$; **, $p<0.01$; ***,

762 p<0.001; ****, p<0.0001; ns, non-significant, using one-way Anova with multiple comparisons.

763

764 **Figure S2. CTPS1 roles in EBV-transformed B-cell growth and survival.**

765 (**A-B**) Immunoblot analysis (top) and growth curve analysis (bottom) of GM11830 LCLs (A)
766 and Mutu I BLs (B) expressing control or independent sgRNAs against CTPS1. WCL were
767 obtained at day 7 post sgRNA expression.

768 **(C)** FACS analysis of 7-AAD uptake in GM11830 LCL (left) or Mutu I BL (right) expressing
769 control or CTPS1 sgRNAs for 7 days.

770 (**D**) Median + SEM values from n=3 replicates, as in C.

771 **(E)** Propidium iodide cell cycle analysis of GM12878 LCL, GM11830, Daudi BL or Mutu I BL
772 expressing control or CTPS1 sgRNAs at Day 9 post sgRNA expression.

773 (**F**) Median + SEM values from n=3 replicates, as in E. Percentages of cells in G2/M, S,
774 G0/G1 or with <2n DNA content indicative of cell death are shown.

775 **(G)** Immunoblot analysis of WCL from GM11830 (left) or Mutu I cells (right) expressing control
776 or CTPS1 sgRNAs for 7 days.

777 Blots in A and G are representative of n = 3 experiments. SEM + Mean values are shown in A,
778 D and F from n=3 replicates. *, p < 0.05; **, p < 0.01; ***, p<0.001; ****, p<0.0001; ns,
779 non-significant using one-way Anova with multiple comparisons.

780

781 **Figure S3. Analysis of CTPS2 roles in EBV-transformed B-cell growth.**

782 **(A)** DepMap CRISPR screen dependency scores (31) for sgRNAs targeting CTPS1 (left) and
783 CTPS2 (right) across cell lines from the indicated cancer cells of origin. Each oval
784 represents the DepMap screen value for a cell line from the tissue indicated at right.
785 Negative values indicates selection against the sgRNAs target the gene over a 21 day
786 growth and survival screen. Values <-1 (red vertical line) indicates cell line dependency on
787 the targeted gene for growth or survival.

788 (**B-C**) Immunoblot analysis (top) and growth curve analysis (bottom) of GM11830 LCL (B) or
789 Mutu I BL (C) expressing control or independent CTPS2 sgRNAs for 7 days.

790 **(D)** FACS analysis of 7-AAD uptake in GM12878 (left) or Daudi cells (right) expressing control
791 or CTPS2 sgRNAs for 7 days.

(E) Median + SEM values from n=3 replicates, as in D, of 7-AAD uptake FACS analysis in GM12878, GM11830, Daudi or Mutu I cells.

(F) Mean + SEM values of FACS propidium iodide cell cycle analysis of GM12878 (left) or Daudi (right) expressing control, CTPS2, CTPS1 or CTPS1/2 sgRNAs for 7 days. Significantly differences from sgControl values are indicated.

Blots in B and C are representative of n = 3 experiments. SEM + Mean values are shown in B-F are from n=3 replicates. *, $p < 0.05$; **, $p < 0.01$; ***, $p<0.001$; ****, $p<0.0001$; ns, non-significant using one-way Anova with multiple comparisons.

Figure S4. Profiling of EBV and immune receptor stimulation effects on UCK1, UCK2 and DHODH expression in primary B-cells.

(A) qPCR analysis of UCK1 and UCK2 mRNA levels in human peripheral blood CD19+ B-cells at the indicated day post infection by B95.8 EBV at MOI=0.1. Day 0 values were set to 1.

(**B**) UCK1, UCK2 and DHODH relative protein abundances from published analyses of tandem-mass-tag-based proteomic analysis at rest and at nine time points after EBV B95.8 infection of human peripheral blood CD19+ B-cells at a multiplicity of infection of 0.1 (28).

(C) qPCR analysis UCK1, UCK2 or DHODH mRNA levels in human peripheral blood CD19+ B-cells stimulated for 24 hours by Mega-CD40L (50ng/mL), CpG (1μM), □IgM crosslinking (1μg/mL), IL-4 (20ng/mL) or combinations thereof, as indicated.

SEM + Mean values are shown in A-C from n=3 replicates. *, $p < 0.05$; **, $p < 0.01$; ***, $p<0.001$; ****, $p<0.0001$; ns, non-significant using one-way Anova with multiple comparisons.

Figure S5. Analysis of DHODH, UCK1/2 and uridine salvage metabolism roles in EBV-transformed B-cell growth.

(A-B) Growth curve analysis of GM11830 (A) or Mutu I (B) expressing control or DHODH sgRNAs and puromycin selected for 48 hours, then grown in media containing uridine-depleted 10% dialyzed fetal bovine serum, in the absence or presence of 200 □M uridine supplementation. Immunoblot analysis of WCL from cells with the indicated sgRNAs are shown to the right.

(C) FACS analysis of 7-AAD abundances in GM12878, GM11830, Mutu I or Daudi expressing the indicated sgRNAs for 7 days and grown in media containing uridine-depleted, dialyzed FBS in the absence or presence of 200 □M uridine supplementation.

(D) Mean + SEM values of FACS analysis of n=3 replicates, as in C.

(E-F) Growth curve analysis (left) and immunoblot of WCL for UCK2 and GAPDH load control or *UCK1* locus T7E1 assay results (right) of GM11830 (E) or Mutu cells (F) expressing the indicated sgRNAs.

Blots in A, B, E and F are representative of n = 3 experiments. SEM + Mean values are shown in A, B, D, E and F from n=3 replicates. *, $p < 0.05$; **, $p < 0.01$; ***, $p<0.001$; ns, non-significant using one-way Anova with multiple comparisons.

Figure 1

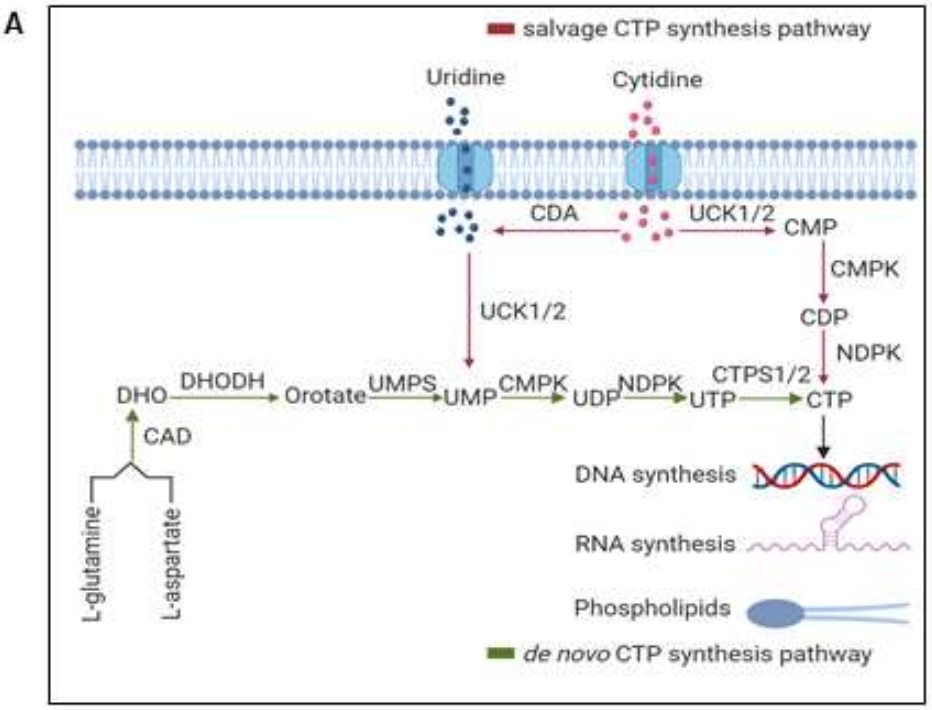
A
salvage CTP synthesis pathway
Uridine
Cytidine
CDA
UCK1/2
CMP
CMPK
CDP
NDPK
UCK1/2
DHO
DHODH
Orotate
UMPS
UMP
CMPK
UDP
NDPK
UTP
CTPS1/2
CTP
CAD
L-glutamine
L-aspartate
DNA synthesis
RNA synthesis
Phospholipids
de novo CTP synthesis pathway

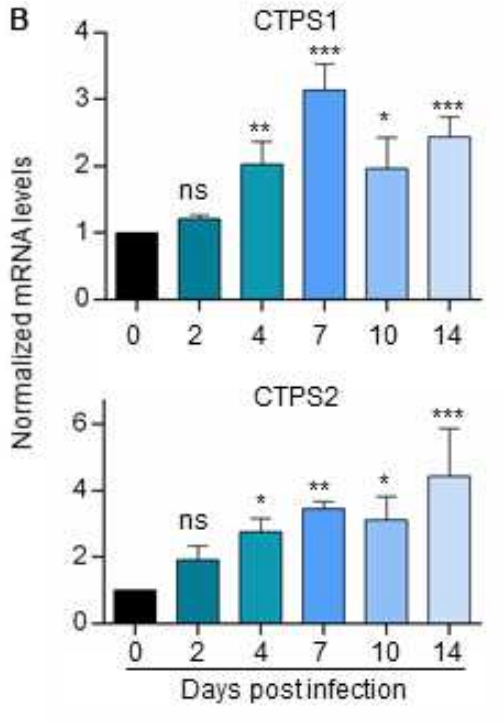
B
CTPS1
CTPS2
Normalized mRNA levels
ns
Days post infection
0
2
4
7
10
14

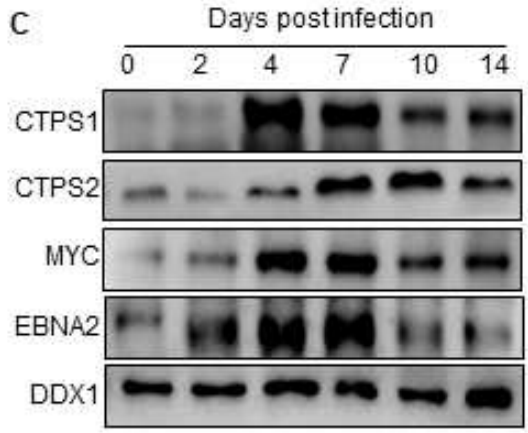
C
Days post infection
0
2
4
7
10
14
CTPS1
CTPS2
MYC
EBNA2
DDX1

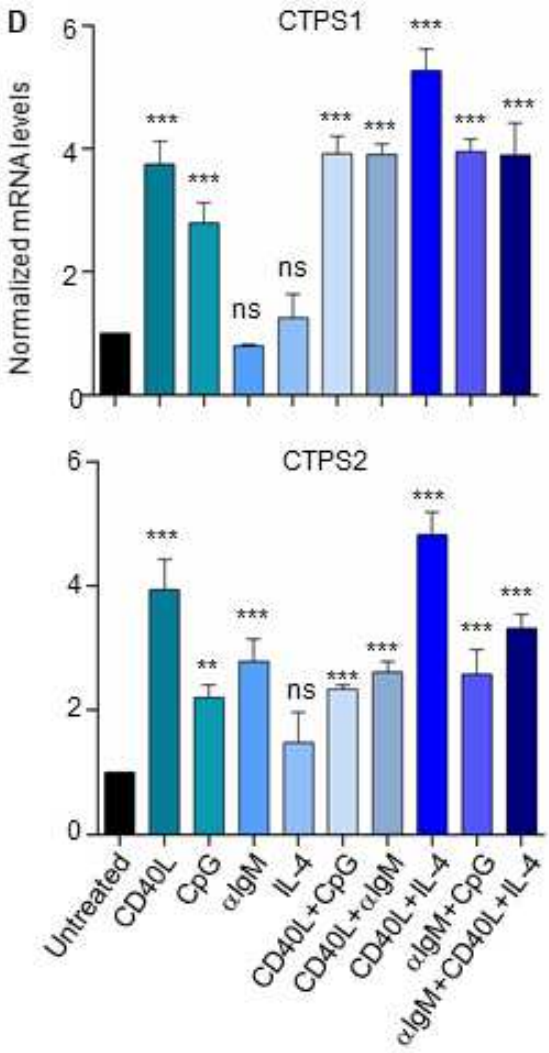
D
CTPS1
CTPS2
Normalized mRNA levels
ns
Untreated
CD40L
CpG
αIgM
IL-4
CD40L+CpG
CD40L+αIgM
CD40L+IL-4
αIgM+CpG
αIgM+CD40L+IL-4

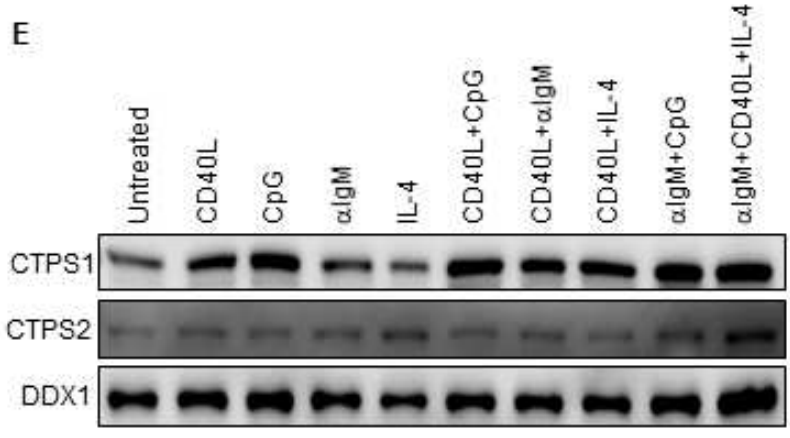
E
Untreated
CD40L
CpG
αIgM
IL-4
CD40L+CpG
CD40L+αIgM
CD40L+IL-4
αIgM+CpG
αIgM+CD40L+IL-4
CTPS1
CTPS2
DDX1

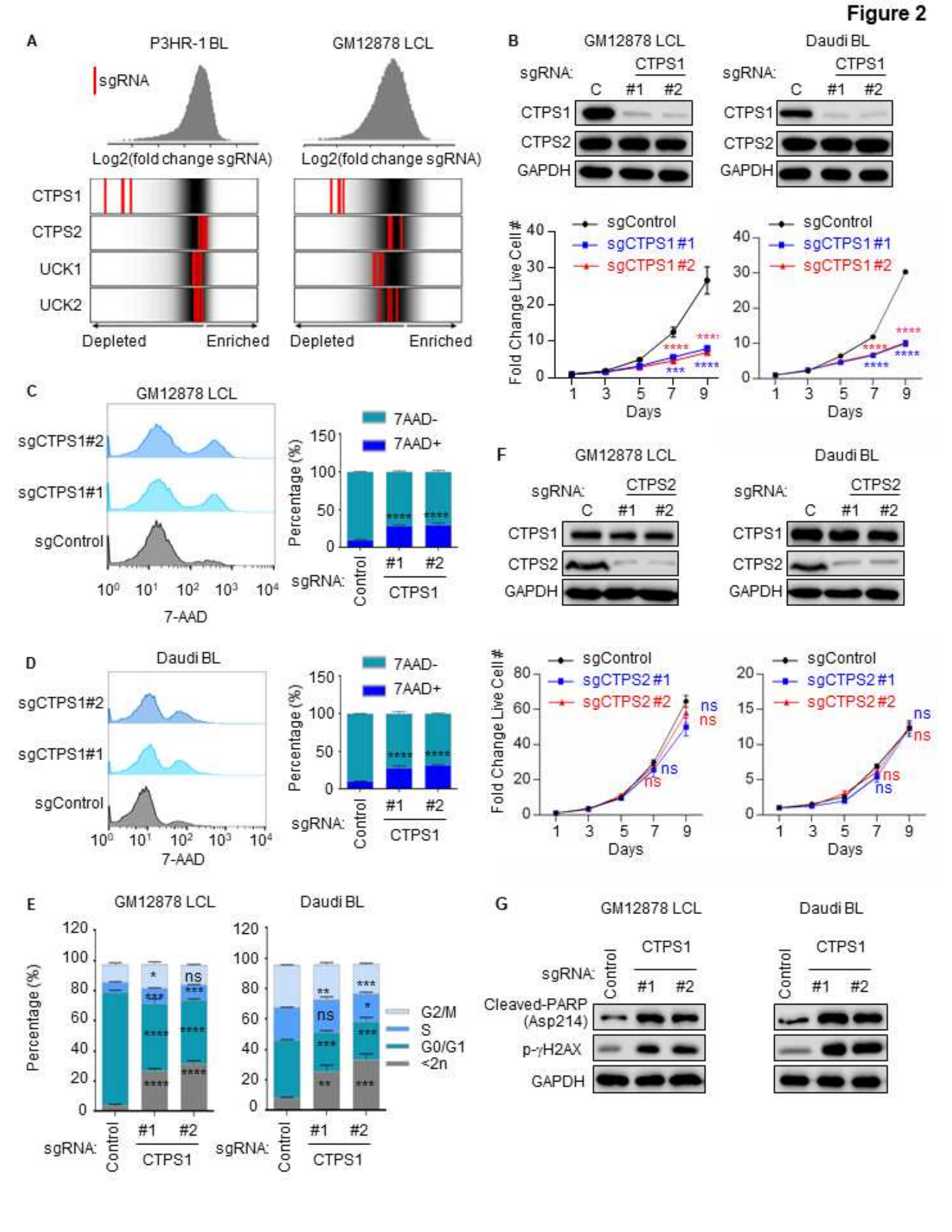
A
P3HR-1 BL
GM12878 LCL
sgRNA
Log2(fold change sgRNA)
Log2(fold change sgRNA)
CTPS1
CTPS2
UCK1
UCK2
Depleted
Enriched
Depleted
Enriched
B
GM12878 LCL
Daudi BL
sgRNA:
CTPS1
C
#1
#2
CTPS1
CTPS2
GAPDH
sgControl
sgCTPS1#1
sgCTPS1#2
Fold Change Live Cell #
Days
C
GM12878 LCL
sgCTPS1#2
sgCTPS1#1
sgControl
7-AAD
7AAD-
7AAD+
Percentage (%)
sgRNA:
Control
CTPS1
D
Daudi BL
F
GM12878 LCL
Daudi BL
CTPS2
sgCTPS2#1
sgCTPS2#2
ns
E
GM12878 LCL
Daudi BL
G2/M
S
G0/G1
<2n
G
GM12878 LCL
Daudi BL
Cleaved-PARP (Asp214)
p-γH2AX

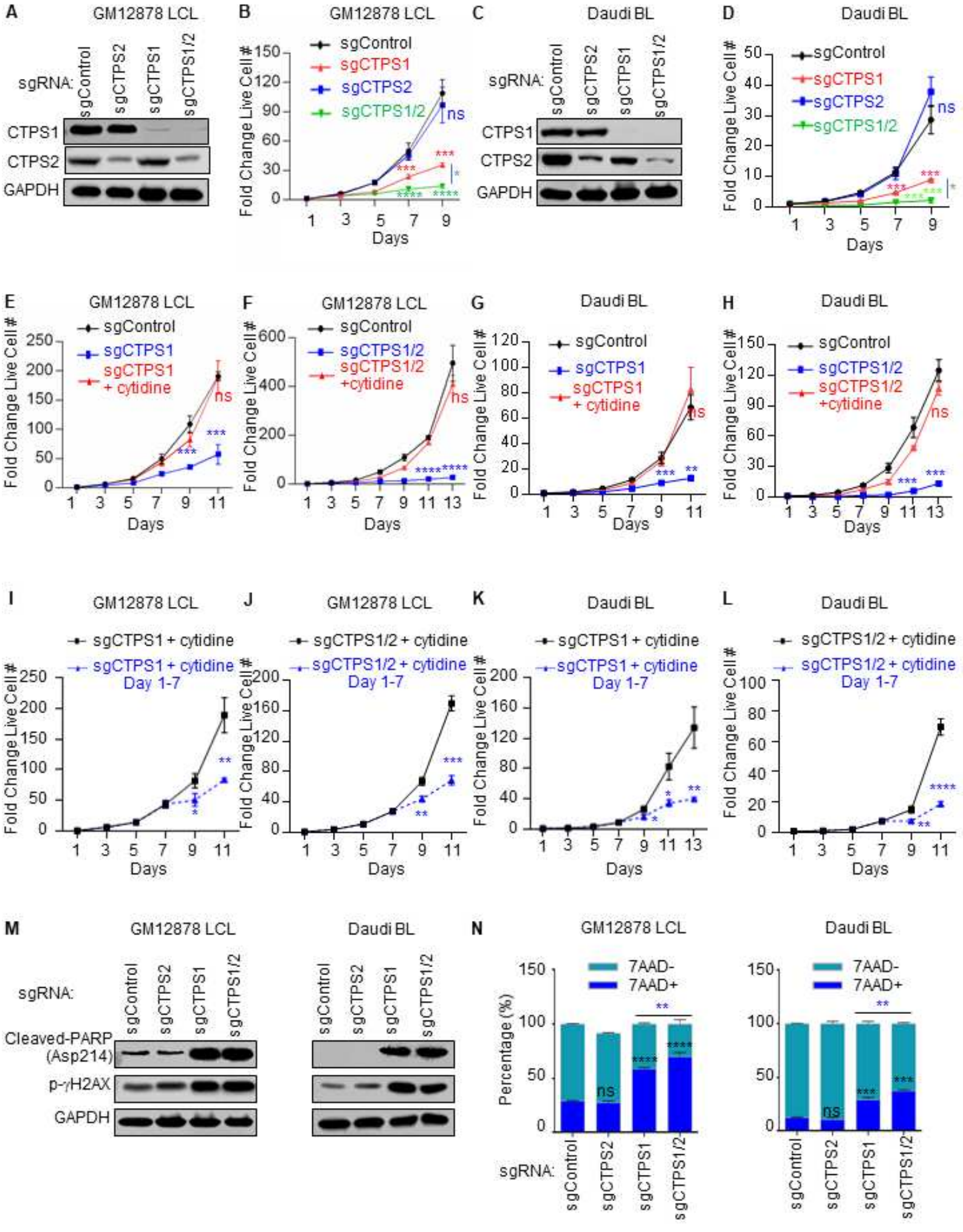
A
GM12878 LCL
sgRNA:
sgControl
sgCTPS2
sgCTPS1
sgCTPS1/2
CTPS1
CTPS2
GAPDH
B
GM12878 LCL
Fold Change Live Cell #
Days
sgControl
sgCTPS1
sgCTPS2
sgCTPS1/2
ns
C
Daudi BL
D
Daudi BL
E
GM12878 LCL
sgControl
sgCTPS1
sgCTPS1 + cytidine
F
GM12878 LCL
sgControl
sgCTPS1/2
sgCTPS1/2 +cytidine
G
Daudi BL
sgControl
sgCTPS1
sgCTPS1 + cytidine
H
Daudi BL
sgControl
sgCTPS1/2
sgCTPS1/2 +cytidine
I
GM12878 LCL
sgCTPS1 + cytidine
sgCTPS1 + cytidine Day 1-7
J
GM12878 LCL
sgCTPS1/2 + cytidine
sgCTPS1/2 + cytidine Day 1-7
K
Daudi BL
sgCTPS1 + cytidine
sgCTPS1 + cytidine Day 1-7
L
Daudi BL
sgCTPS1/2 + cytidine
sgCTPS1/2 + cytidine Day 1-7
M
GM12878 LCL
Daudi BL
sgRNA:
sgControl
sgCTPS2
sgCTPS1
sgCTPS1/2
Cleaved-PARP (Asp214)
p-γH2AX
GAPDH
N
GM12878 LCL
Daudi BL
7AAD-
7AAD+
Percentage (%)
sgRNA:
sgControl
sgCTPS2
sgCTPS1
sgCTPS1/2

Figure 4

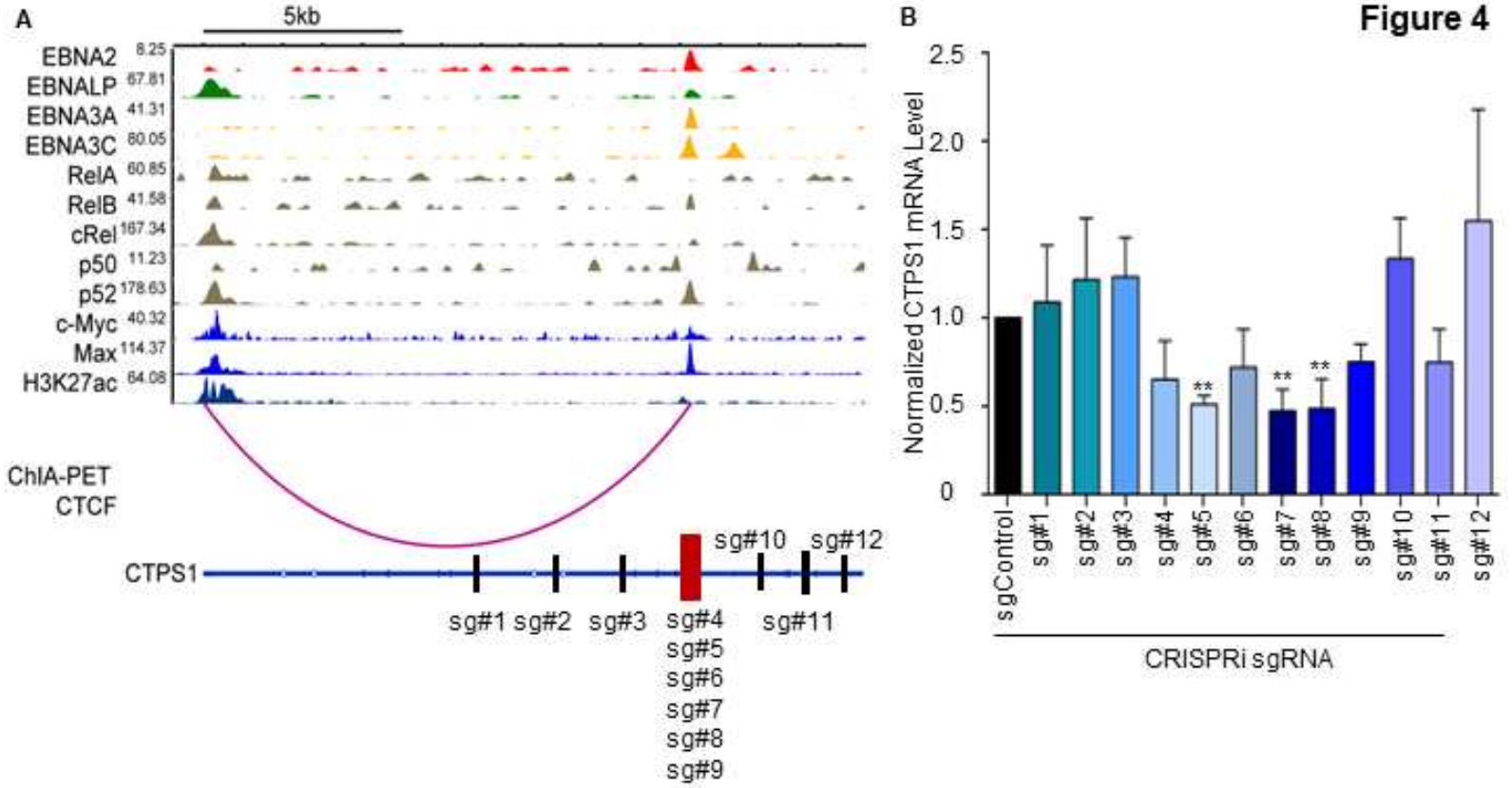
A
5kb
EBNA2
EBNALP
EBNA3A
EBNA3C
RelA
RelB
cRel
p50
p52
c-Myc
Max
H3K27ac
ChIA-PET
CTCF
CTPS1
sg#1 sg#2 sg#3 sg#4 sg#5 sg#6 sg#7 sg#8 sg#9 sg#10 sg#11 sg#12
B
Normalized CTPS1 mRNA Level
sgControl
CRISPRi sgRNA

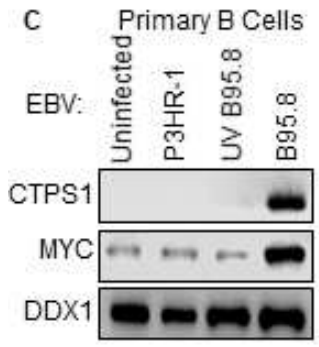
C
Primary B Cells
EBV:
Uninfected
P3HR-1
UV B95.8
B95.8
CTPS1
MYC
DDX1

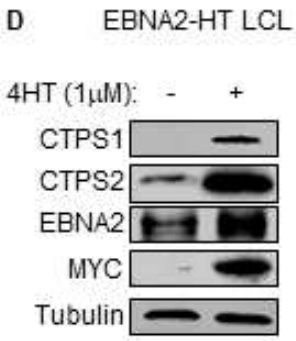
D
EBNA2-HT LCL
4HT (1μM):
CTPS1
CTPS2
EBNA2
MYC
Tubulin

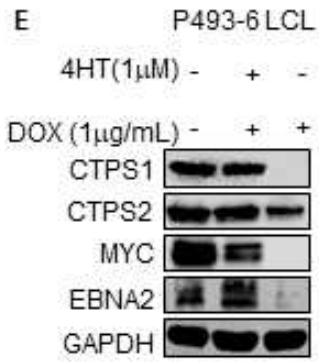
E
P493-6 LCL
4HT(1μM)
DOX (1μg/mL)
CTPS1
CTPS2
MYC
EBNA2
GAPDH

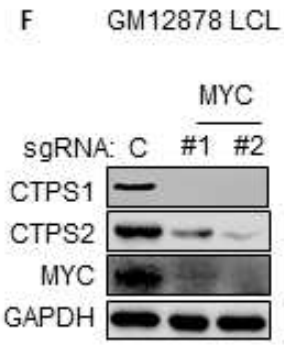
F
GM12878 LCL
MYC
sgRNA: C #1 #2
CTPS1
CTPS2
MYC
GAPDH

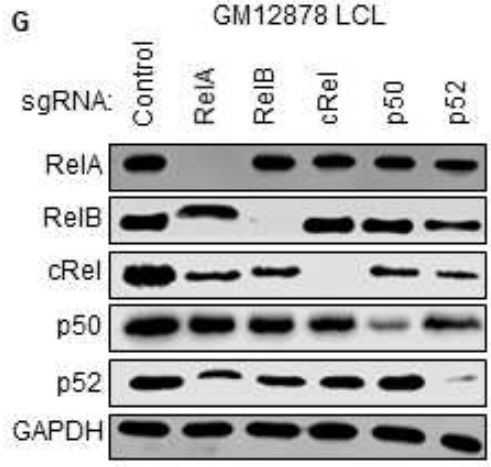
G
GM12878 LCL
sgRNA:
Control
RelA
RelB
cRel
p50
p52
GAPDH

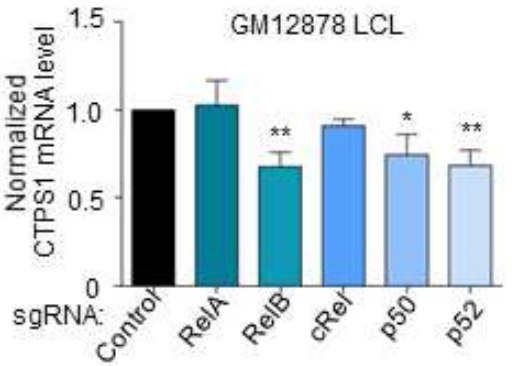
H
GM12878 LCL
Normalized CTPS1 mRNA level
sgRNA:
Control
RelA
RelB
cRel
p50
p52

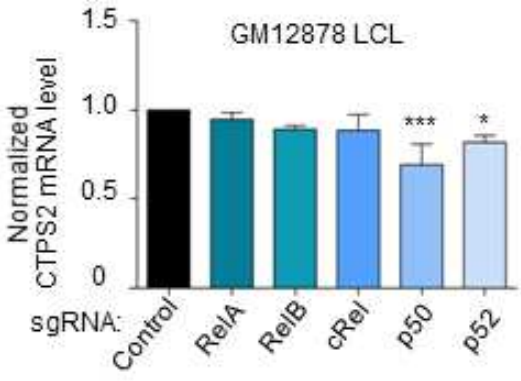
GM12878 LCL
Normalized CTPS2 mRNA level
sgRNA:
Control
RelA
RelB
cRel
p50
p52

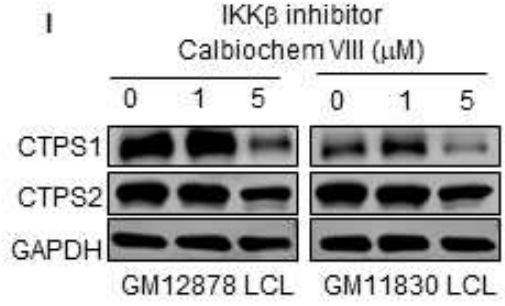
I
IKKβ inhibitor
Calbiochem VIII (μM)
0 1 5 0 1 5
CTPS1
CTPS2
GAPDH
GM12878 LCL
GM11830 LCL

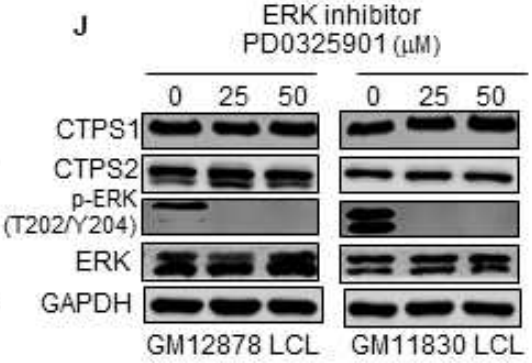
J
ERK inhibitor
PD0325901 (μM)
0 25 50 0 25 50
CTPS1
CTPS2
p-ERK
(T202/Y204)
ERK
GAPDH
GM12878 LCL
GM11830 LCL

Figure 5

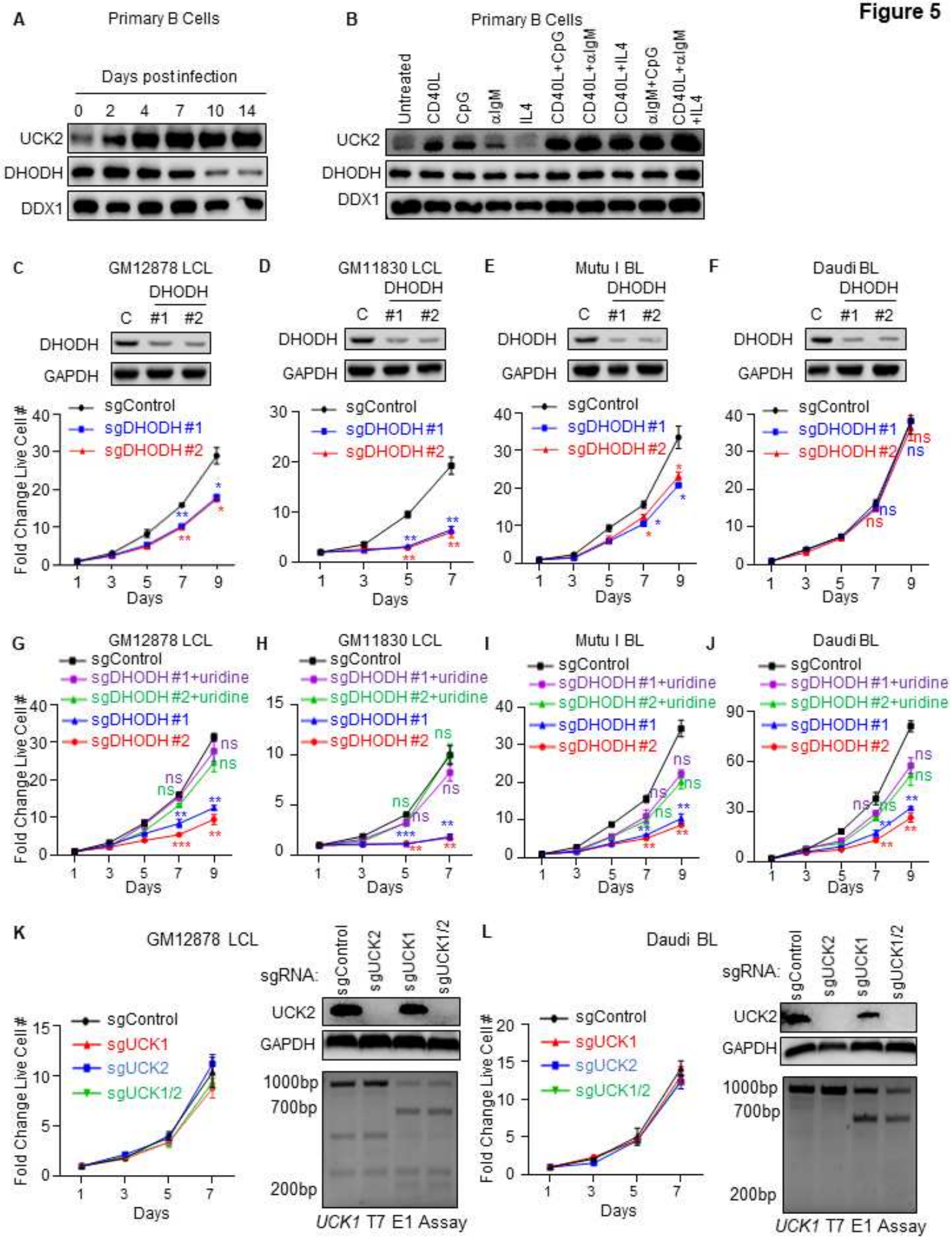
A
Primary B Cells
Days post infection
0 2 4 7 10 14
UCK2
DHODH
DDX1
B
Primary B Cells
Untreated
CD40L
CpG
αIgM
IL4
CD40L+CpG
CD40L+αIgM
CD40L+IL4
αIgM+CpG
CD40L+αIgM +IL4
UCK2
DHODH
DDX1
C
GM12878 LCL
DHODH
C #1 #2
DHODH
GAPDH
sgControl
sgDHODH#1
sgDHODH#2
Fold Change Live Cell #
Days
D
GM11830 LCL
E
Mutu I BL
F
Daudi BL
G
GM12878 LCL
sgDHODH#1+uridine
sgDHODH#2+uridine
H
GM11830 LCL
I
Mutu I BL
J
Daudi BL
K
GM12878 LCL
sgRNA:
sgControl
sgUCK2
sgUCK1
sgUCK1/2
UCK2
GAPDH
1000bp
700bp
200bp
UCK1 T7 E1 Assay
L
Daudi BL

Figure 6

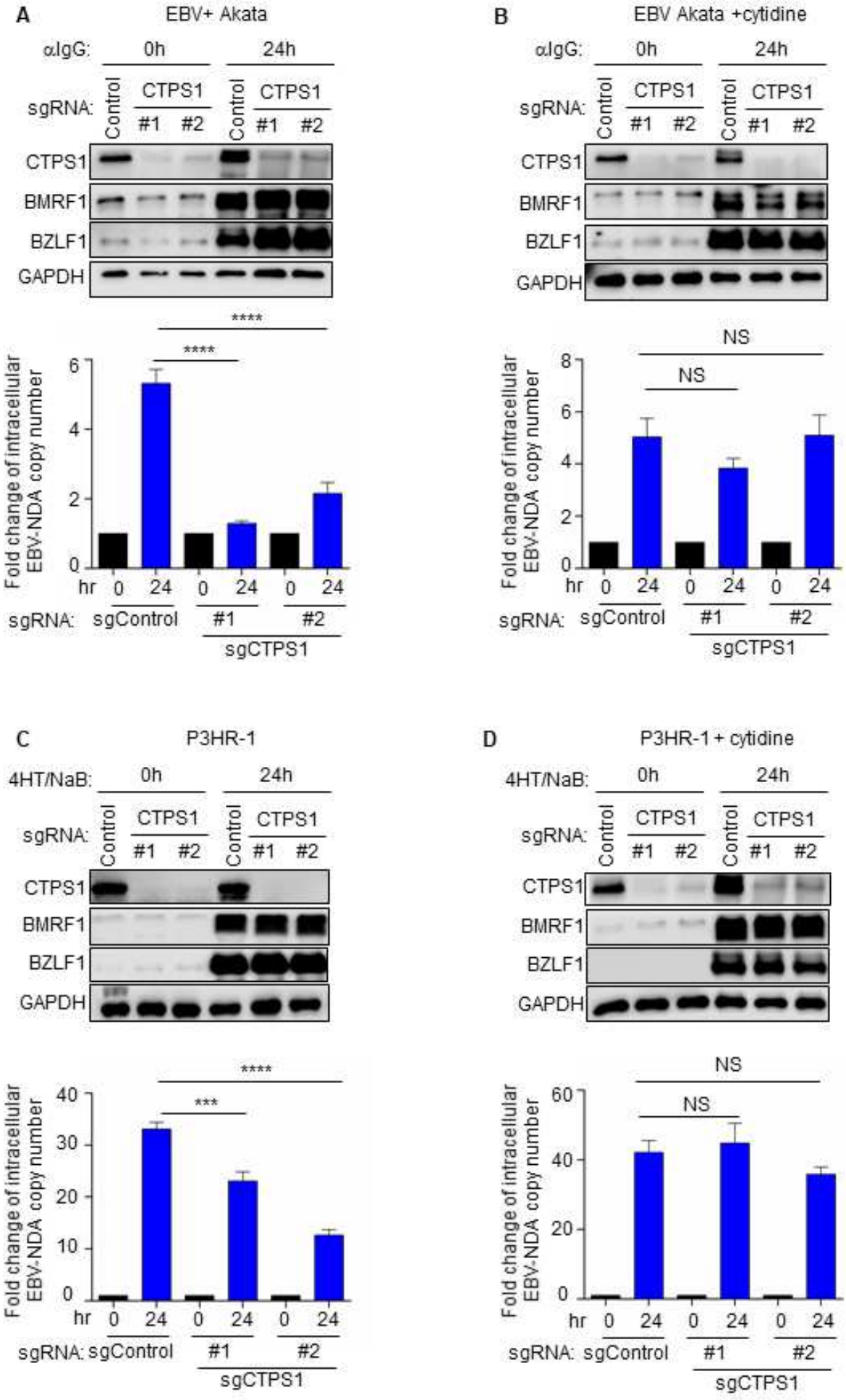
A
EBV+ Akata
αIgG:
0h
24h
sgRNA:
Control
CTPS1 #1
CTPS1 #2
CTPS1
BMRF1
BZLF1
GAPDH
****
****
Fold change of intracellular EBV-NDA copy number
hr
sgRNA:
sgControl
sgCTPS1
B
EBV Akata +cytidine
NS
NS
C
P3HR-1
4HT/NaB:
***
D
P3HR-1 + cytidine

Figure 7

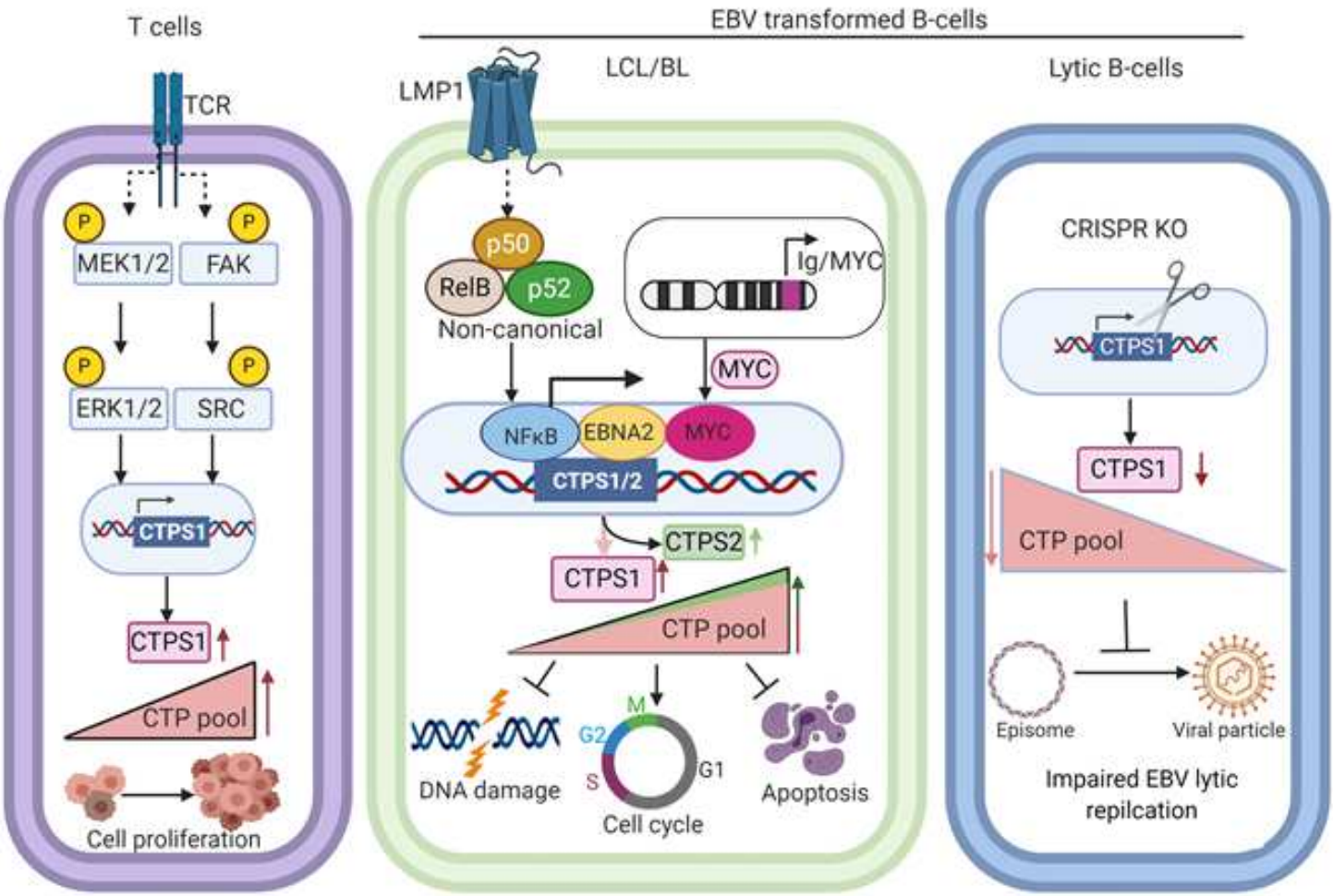
T cells
TCR
P
MEK1/2
FAK
ERK1/2
SRC
CTPS1
CTPS1
CTP pool
Cell proliferation
EBV transformed B-cells
LCL/BL
LMP1
p50
RelB
p52
Non-canonical
Ig/MYC
MYC
NFκB
EBNA2
MYC
CTPS1/2
CTPS2
CTPS1
CTP pool
DNA damage
M
G2
S
G1
Cell cycle
Apoptosis
Lytic B-cells
CRISPR KO
CTPS1
CTPS1
CTP pool
Episome
Viral particle
Impaired EBV lytic repilcation